INFN
Istituto Nazionale
di Fisica Nucleare
SEZIONE DI MILANO
Laboratorio Acceleratori e Superconduttività Applicata

NED

STUDY OF THE QUENCH PROPAGATION AND OF THE PROTECTION SYSTEM OF THE COS-THETA NED DIPOLE PROTOTYPE

8 November, 2005

V. Granata, M. Sorbi, G. Volpini, D. Zamborlin
INFN – LASA and Milan University, via fratelli Cervi 2001, 20090 Segrate MI - Italy

In this report we present our studies of the propagation of the quench in the NED dipole prototype, to derive a preliminary configuration of the protection system of the magnet (quench protection heaters, dump resistors, etc.). The simulations have been performed by using the code QLASA [1]. In this code, the geometry of the magnet is simplified to a series of solenoidal concentric magnets and the evolution of the quench is calculated with the Wilson's approach [2]. An analogous study has been performed with the CERN code QUABER [3],[4], and the results are discussed in section 3.

1. MAIN CHARACTERISTICS OF DIPOLE MAGNET

The reference mechanical and magnetic baseline design of the magnet is described in paragraph 3.4 of [5]. Fig. 1 shows a quadrant of the cross section of the magnet. It is a classical "cosθ" type magnet, with two layers. The bore diameter is 88 mm. For simplicity and economical reasons, both layers are wound with the same conductor. The number of turns is 38 for the inner layer and 52 for the outer layer.

The chosen cable is referred to as CK6. The main geometrical and superconducting characteristics are reported in Table I:

Table I : Salient geometrical and superconducting parameters of the conductor.

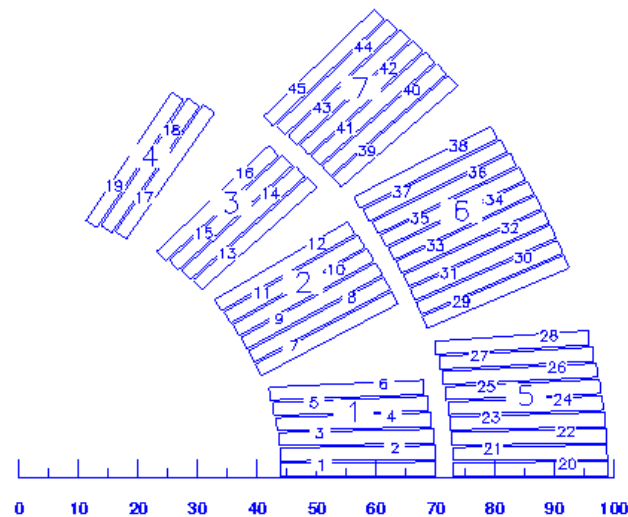| cable name	strand diam. [mm]	strand number	Cu/non_Cu	height [mm]	width inner [mm]	width outer [mm]	insulation thickness [mm]	Jc_strand @ 15T, 4.2K [A/mm^2]	Jc_cable @ 15T, 4.2K [A/mm^2]
CK6	1.25	40	1.38	26	2.175	2.375	0.2	666.67	417.1

Fig. 1. Magnet cross section (design CK6)

The material composition for each strand is reported in Table II, while Table III reports the percentage composition of the Rutherford cable, with the insulation. It is assumed that the space between the strands is completely filled by the insulation, *i.e.*, epoxy impregnated fiber glass. In the simulations, the thermal and electrical properties of G10 have been used for the insulation.

Table II : Material composition of each strand of conductor CK6. Percentages by volume.

Copper	58%
Bronze	20%
Nb$_3$Sn	11%
Tin	6%
Tantalum	5%

Table III : Material composition of insulated Rutherford cable CK6. Percentages by volume.

Copper	39%
Bronze	13%
Nb$_3$Sn	7%
Tin	4%
Tantalum	3%
G10	34%

In the magnet, angular wedges are foreseen between the blocks of each layer. These spacers will be made up of a copper-aluminium alloy, but from a point of view of material properties, they are treated as copper with a low RRR. In the simulations with QLASA, these spacers are included in the magnet geometry and, because the magnet is supposed to be a homogeneous and anisotropic medium, the spacers are not localized at their own positions but are spreaded over the magnet volume.

For quench studies, three magnet lengths have been considered: 1 m long, 5 m long and 10 m long, with the same cross section for all magnets.

In the simulation with QLASA, the magnet is made up of two separate solenoids: the first solenoid represents the inner layer and the second solenoid represents the outer layer. The average circumference of each solenoid (calculated as the average between the circumferences at the external and internal radii) is equal to the average length of the corresponding layer of the magnet,

2

the thickness of the solenoid is equal to the layer thickness and its height is equal to the azimuthal length of the arcs assumed by the layers.

Table IV presents the material percentages of the layer-solenoids used in the simulation. The composition is slightly different between layer 1 and layer 2 because the volumetric occupation of the spacers is not in the same ratio for both the layers.

Table IV : Material composition of the two layers in the simulations. Percentages by volume.

First layer		Second layer	
Copper	34 %	Copper	34%
Nb_3Sn	6 %	Nb_3Sn	6%
Tantalum	3 %	Tantalum	3%
Bronze	12 %	Bronze	11%
G10	31 %	G10	31%
Tin	4 %	Tin	3%
Spacer	10 %	Spacer	12%

The operating current of the magnet is 28860 A, the total current is 2.60 MAt and the operating temperature is set to 4.2 K.

Figure 2 shows a map of the magnetic field on the conductors at the maximum current value, calculated by Roxie [5].
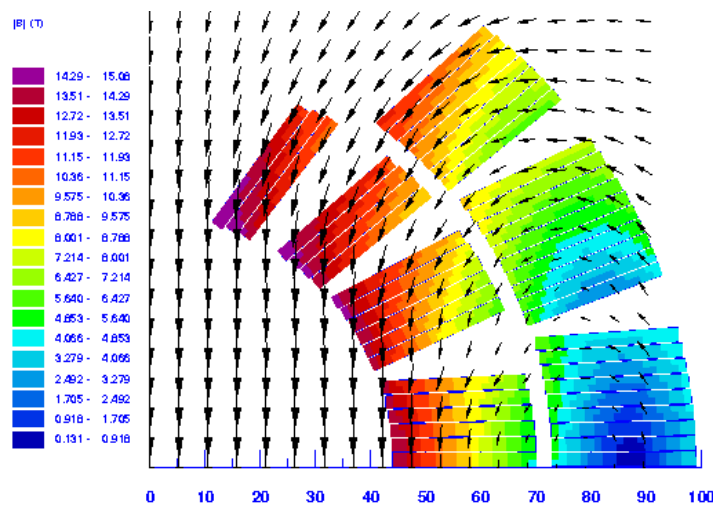

Fig. 2 : Field map on the conductors

In the quench simulation, the magnetic field is calculated with a linear interpolation between 4 assigned values at 4 points of each solenoid, as described in Fig. 3. The values of the assigned fields at the maximum current are reported in Table V.
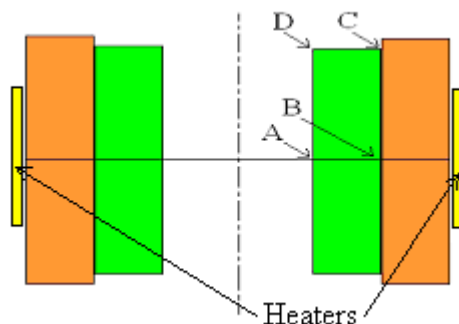
Fig. 3 : Cross section, along the symmetry axis, of the solenoids which simulate the dipole coils. The four points A, B, C, D in the solenoids where the field is pre-assigned are shown. At the other points, the field is linearly interpolated.

Table V : Values of the pre-assigned magnetic field at the points reported in Fig. 3 (for I=28860 A).

	A	B	C	D
Layer 1	13.90 T	4.45 T	12.32 T	15.00 T
Layer 2	4.45 T	3.67 T	9.82 T	12.32 T

The electrical circuit of the magnet is sketched in Fig. 4. It includes the four windings that compose the magnet (the outer-up, inner-up, inner-down and outer down windings) connected in series, a dump resistor, the power supply and the main switch. The ground connection is in one of the terminal of the power supply. The opening of the main switch of the power supply is driven by the Quench Detection System (QDS). In the simulation the threshold voltage that triggers the QDS is set at 10 mV. After the resistive threshold voltage has been reached, it is assumed that a delay occurs before the main switch is completely opened. The criticality of this delay time and of the value of the dump resistor has been studied, and the results are reported in the oncoming paragraphs.
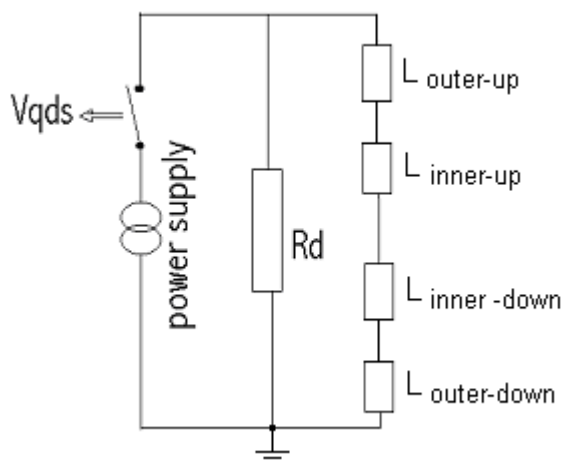

Fig. 4 : Electrical circuit of the magnet.

The total inductance of the magnet has been calculated by [5] and is 4.5 mH/m. The inductance of the outer and inner sections and their mutual inductances have been determined by taking intp account the number of turns per layer and the different surfaces embraced by the layers. The self inductance of the two outer windings (up and down) and their mutual inductances with the inner layer have been obtained by dividing into two equal parts the inductance of the outer layer and the

mutual inductance between the inner and outer layer. The inductance and the mutual inductances of the two inner windings have been calculated in the same way. This seemingly rough subdivision of the self and mutual inductances of the up and down windings is correct for the voltage drop evaluation, because all the windings are connected in series and the current is the same in all the coils. Table VI reports the main electrical characteristics of the magnet.

Table VI : Salient electrical parameters of dipole magnet.

Total self inductance inner layer	0.876 mH/m
Total self inductance outer layer	1.71 mH/m
Mutual inductance between layers	0.976 mH/m
Operating current	28660 A
Stored magnetic energy	1.86 MJ/m

2. MAIN SIMULATIONS RESULTS

The physical quantities computed in the simulations are: the hot spot temperature, the maximum voltage of the whole magnet and the maximum voltage of each winding.
The total energy stored in the magnet is 1.86 MJ/m. If we assume that the quench spreads through the magnet instantaneously and no energy is extracted, the inner layer reaches an uniform temperature of about 100 K, and the outer layer about 125 K. These reference values indicate that we will have to face temperatures well above 100 K. Fig. 5 displays MIIT's curves calculated using data from different material libraries [6]. Several curves are represented, corresponding to different sources of material properties for copper and G10. It appears that the differences are quite modest.
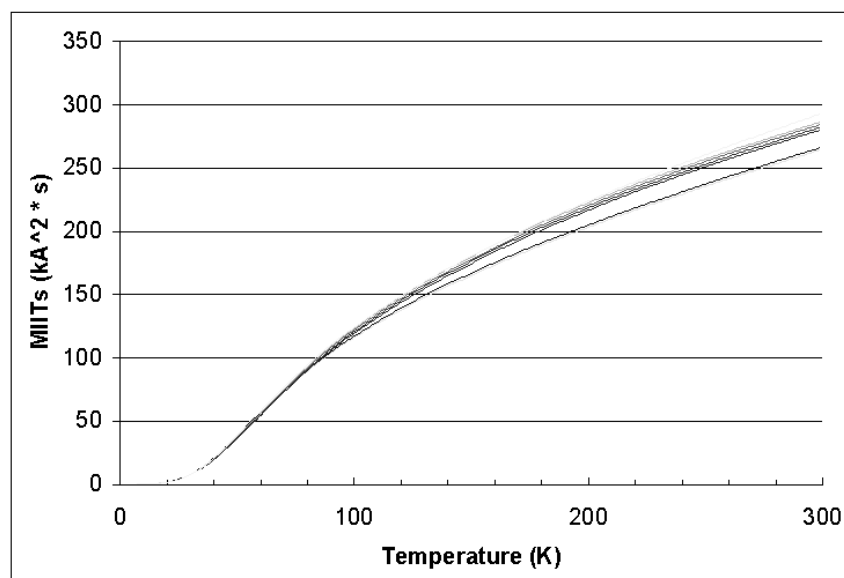

Fig. 5 : MIIT's curves computed using data from different material libraries.

2.1. 1-m-long prototype
The study of the 1 m long prototype has been done without the presence of quench heaters. In fact, since the inductance is sufficiently low, it is possible to extract a significant part of the magnetic energy by means of the dump resistor. The quench is supposed to originate in the zone with the peak field (point D in Fig. 3) and to spread over the entire magnet. Fig. 6 displays the percentage of extracted energy vs. value of the dump resistor. Fig. 7 and Fig. 8 represent respectively the

maximum voltage and the hot spot temperature in each layer vs. the value of dump resistor. The delay between the quench detection and the opening of the main switch is 40 ms.
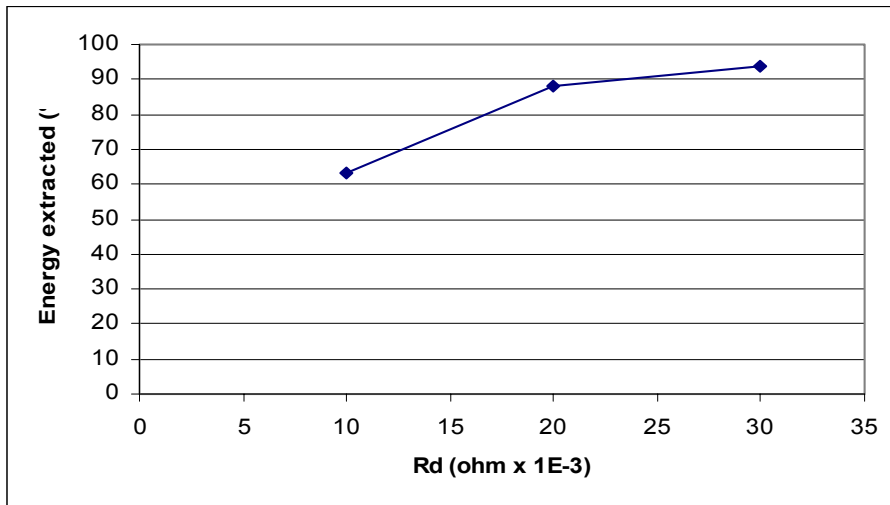

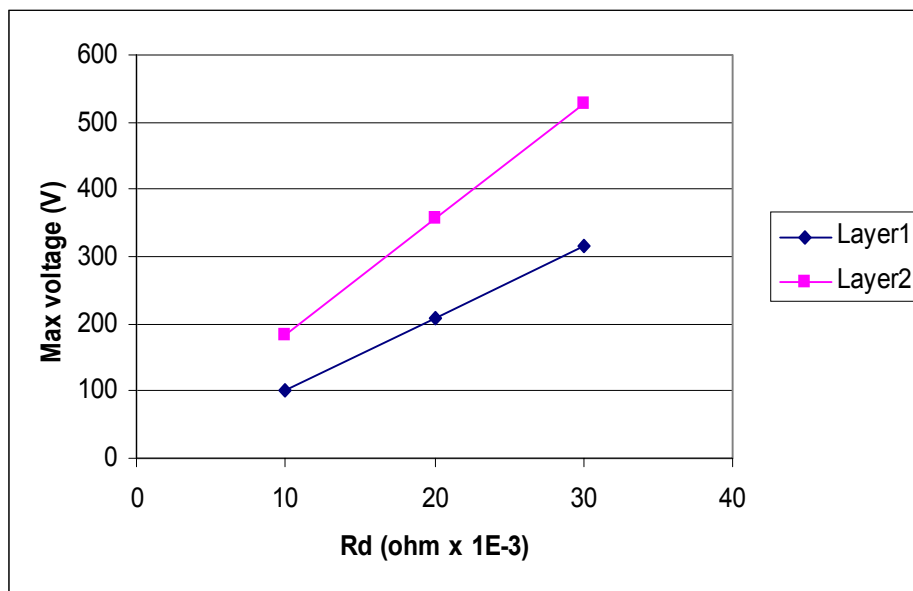Fig. 6 : 1-m-long prototype: percentage of extracted energy vs. value of dump resistor.

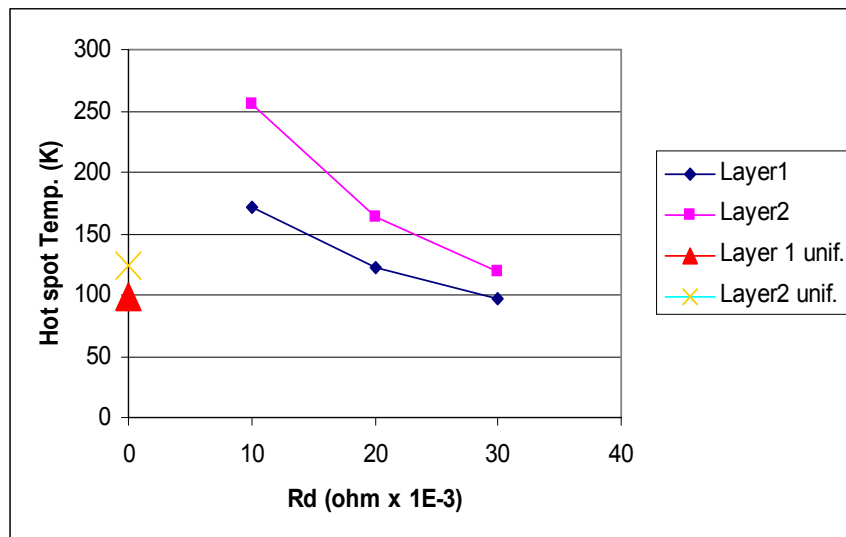Fig. 7 : 1-m-long prototype: maximum voltage in each layer vs. value of dump resistor.

Fig. 8 : 1-m-long prototype: hot spot temperature on each layer vs. value of dump resistor.

2.2. 5-m-long prototype

The study of the quench in the 5-m-long prototype has been performed considering the presence of quench heaters. Indeed in this case the total energy of the magnet is 5 times higher than in the case of a 1-m-long prototype, and the energy extracted by the dump resistor represents a small fraction of the total energy.

The quench heaters are supposed to be glued onto the external surface of the outer layer (see Fig. 3). They are 5 cm high and their length has been varied in order to see its influence on the magnet protection.

The dynamic of the quench can be summarized as follows:

1. At time t=0 a spontaneous quench starts in the maximum field zone of the inner layer (point D of Fig. 3).
2. After a few milliseconds, the QDS detects a resistive voltage (a few tens of millivolt) across the magnet, which is recognized as a quench.
3. After a delay time, the main switch of the power supply is opened and the quench heaters are assumed to induce an extended quench in the outer layer of the magnet. The influence of this delay time on the quench development is studied. If it is not differently specified, the delay times between the quench detection and the switching off of the power supply is the same of the delay time between the quench detection and beginning of new quenches induced by the heaters.
4. When the quench produced by the heaters in the outer layers reaches the boundary of the inner layer, a new extended quench is assumed to start in the inner windings.

Several simulations have been performed, in order to determine the optimal value of dump resistor and the influence of the delay time, heater length and operating current on the quench development. The limit chosen for the maximum voltage in the magnet is 800 V, and the maximum allowable temperature is 300 K. The result of this parametric study is summarized in the following paragraphs. In Appendix A the evolution of current, hot spot temperature and voltages are reported for different values of dump resistors.

2.2.1. Influence of dump resistor

When increasing the dump resistor, the energy dissipated externally to the magnet increases, so that the hot spot temperature on each coil diminishes, and the total voltage increases. This influence is well described in Figs. 9, 10 and 11, where the fractions of dissipated energy in the magnet, the hot spot temperatures and the maximum voltages are represented as a function of dump resistor value. In the simulations, the following parameters have been kept constant:

7

Detection threshold voltage= 10 mV
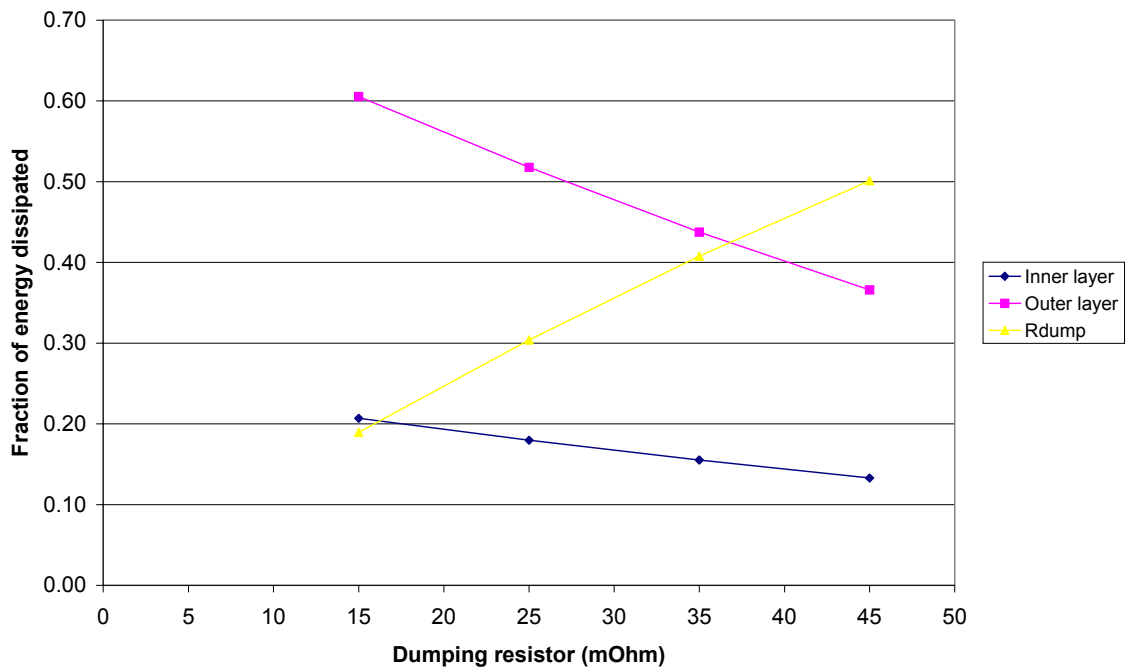Delay time = 30 ms
Heaters length = 5 m

Fig. 9 : Fraction of energy dissipated in each layer and in the dump resistor vs. value of dump resistor.
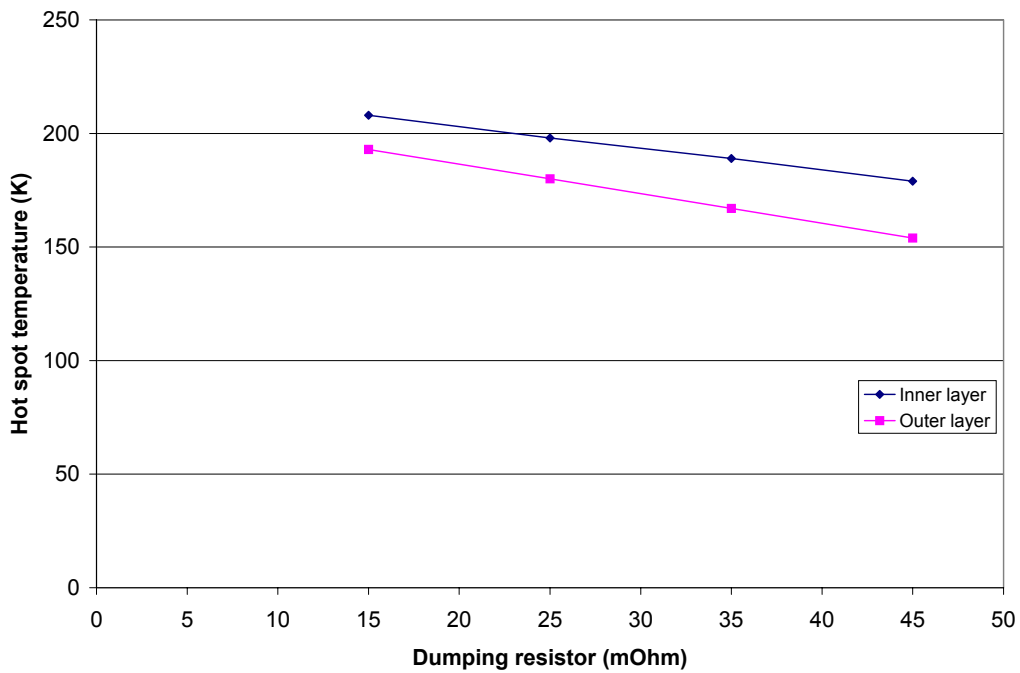

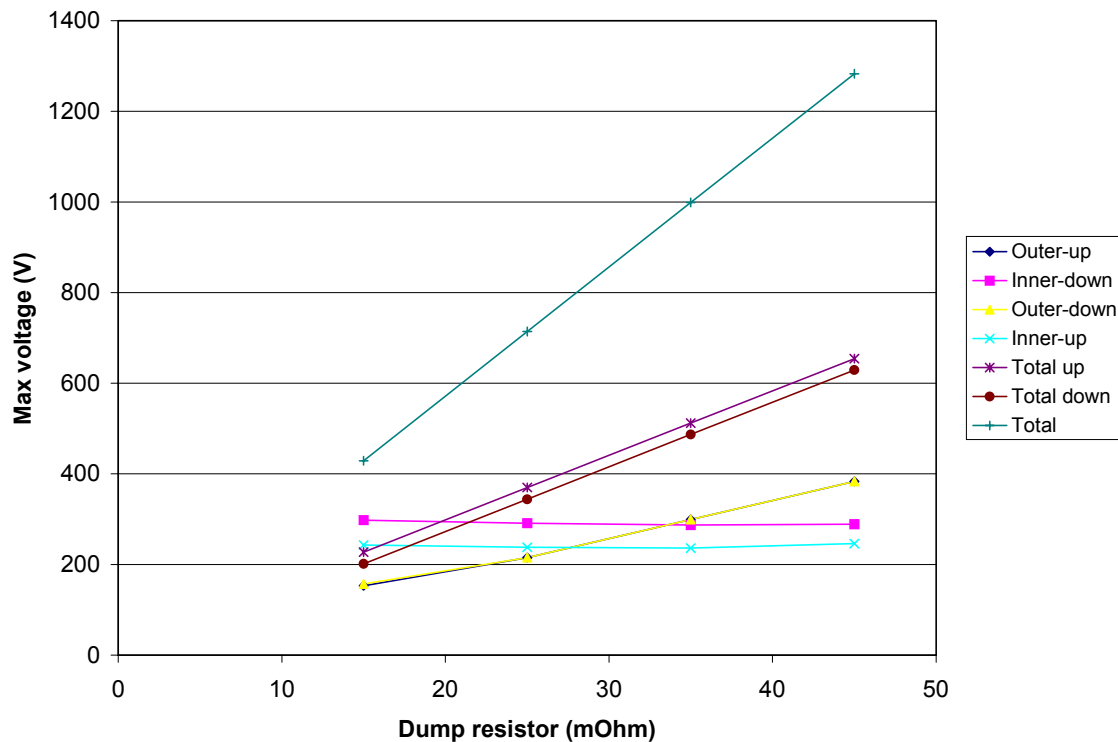Fig. 10 : Hot spot temperature in each layer vs. value of dump resistor.

Fig. : 11 Maximum voltage across each winding and across the whole magnet vs. value of dump resistor.

It appears that the maximum admittable voltage across the magnet sets an upper limit to the value of the dump resistor. In order to keep this voltage below 800 V, we need to choose a dump resistor of 25 mohm or less.

2.2.2 Influence of delay time

This delay corresponds to the time that, from the detection of a spontaneous quench in the inner layer, the protection device takes to switch off the power supply and to initiate extended quenches on the outer layers by means of the heaters. The longer this time, the larger the dissipated energy in the inner layer, and the greater the hot spot temperature of this layer. This behaviour can be observed in Fig. 12, where the hot spot temperature vs. the delay time is represented. Fig. 13 displays maximum voltage vs. delay time. In this case the maximum voltage in the inner layer decreases when the delay time increases because the voltage is dominated by the inductive component (which is negative), and consequently, as the delay time increases, the resistive voltage will partially compensate the inductive voltage. In the simulations the following values have been kept constant:

     Detection threshold voltage= 10 mV
     Dump resistor = 25 mohm
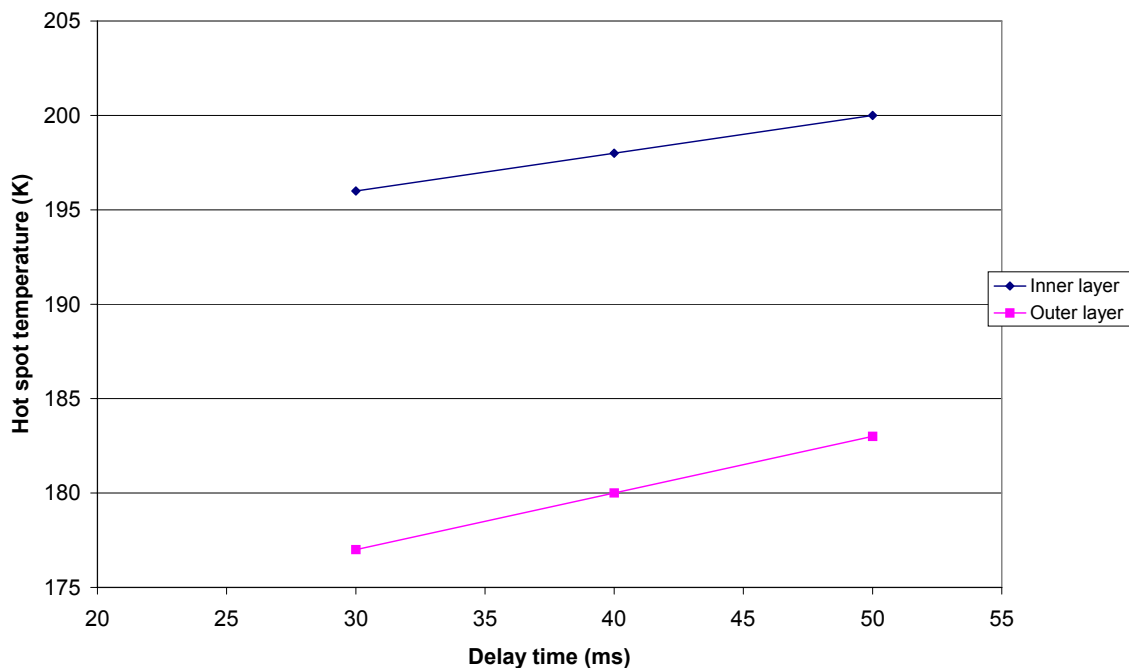   Heaters length = 5 m

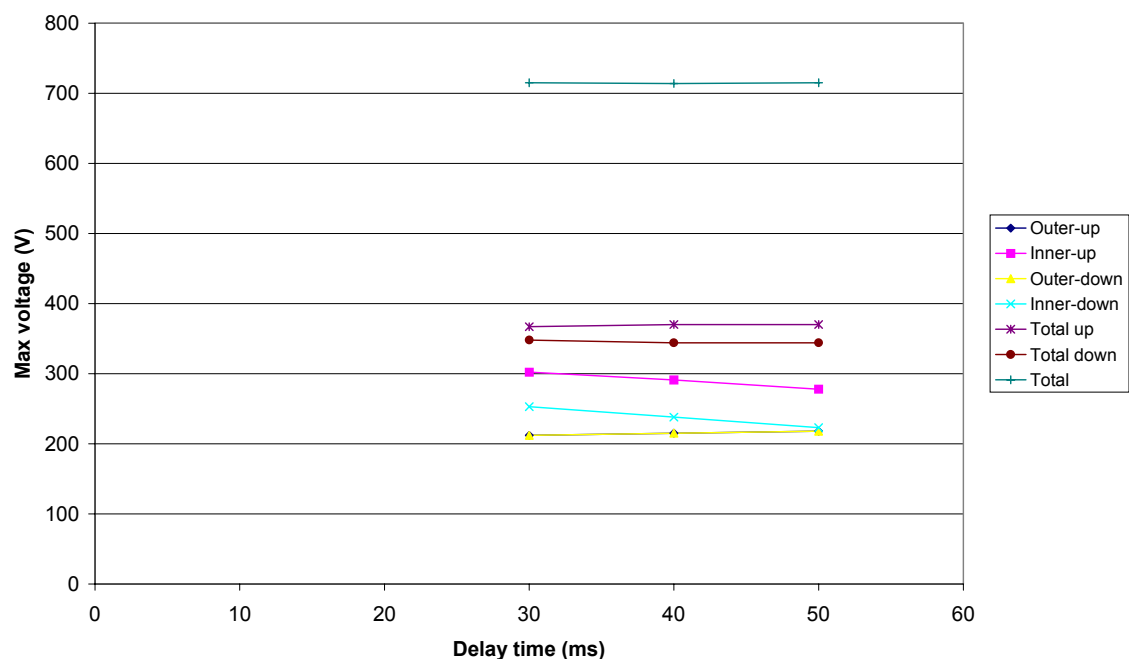Fig. 12 : Hot spot temperature in each layer vs. the delay time.

Fig. 13 : Maximum voltage in each layer and in the whole magnet vs. the delay time.

From this analysis we can conclude that the delay time is not a critical parameter for the protection of the magnet. In the following, we shall set this delay to 40 ms, which is a typical value for accelerator magnet.

2.2.3 Influence of quench-heaters length

The effective length of the quench heaters is an important parameter because it controls the rapidity with which the quench spreads in the outer layer and in the whole magnet. Fig. 14 and Fig. 15 display hot spot temperature and maximum voltage vs. quench heater length. The hot spot

temperature is quite sensitive to heater length, which should be at least 3 m long. In the simulations the following values have been kept constant:

        Detection threshold voltage= 10 mV

        Dump resistor = 25 mohm
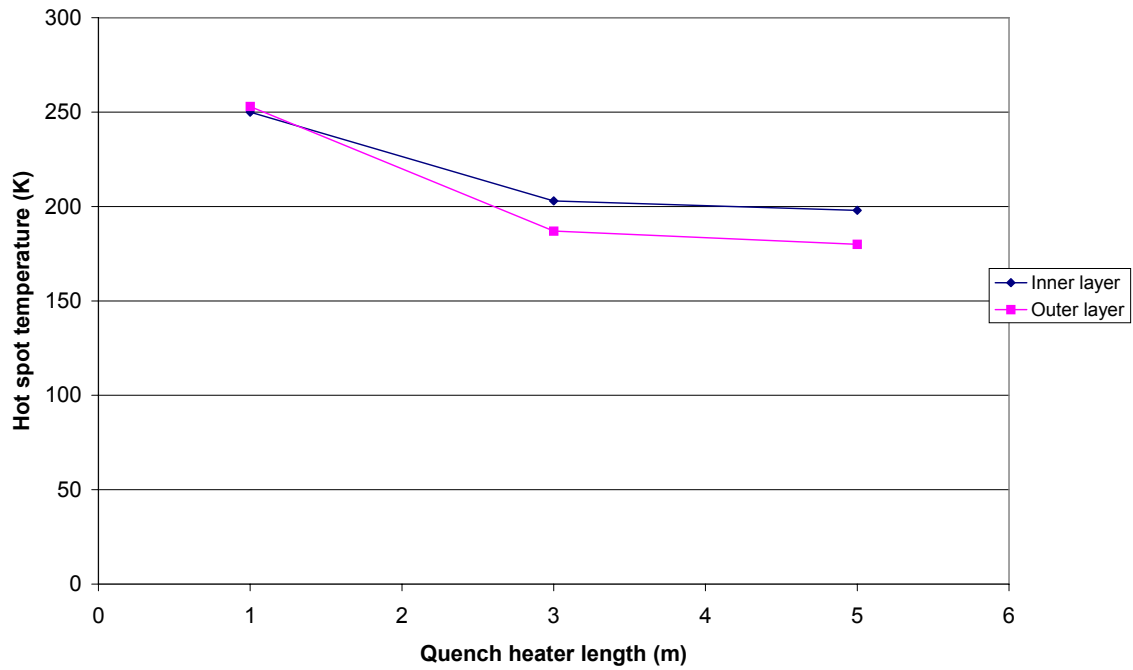
        Delay time = 40 ms

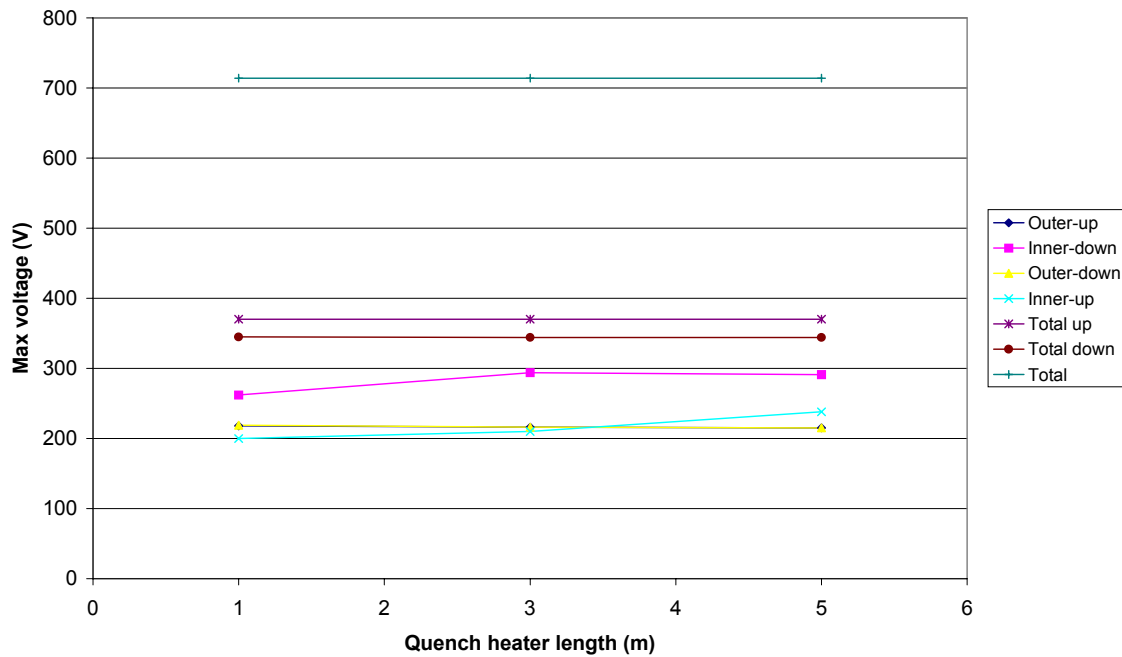Fig. 14 : Hot spot temperature in each layers vs. quench-heaters length.

Fig. 15 : Maximum voltage in each layer and in the whole magnet vs. quench-heater length.

2.2.4 Influence of operating current

In the model used to compute the quench propagation velocity, the quench velocity is very dependent on the operating current of the magnet. In particular the propagation velocity decreases as the current decreases. On the other hand, also the magnetic stored energy is very dependent by the operating current. For this reason it is necessary to verify whether the critical parameters (hot spot temperature and maximum voltage) become critical at lower values of the current. Moreover, at low value of current, the time necessary for the quench heaters to initiate a quench increases significantly, because the current sharing temperature of the conductor is higher at lower current, and consequently it is necessary to set a different delay time for the heaters.

We assumed that the delay time is directly proportional to the current sharing temperature of the conductor. Table VII summarizes, for different operating current values, the corresponding values of current sharing temperature of the outer layer (for the peak field zone), the delay time for the quench heaters and the longitudinal quench velocity for both layers (maximum values). The current sharing temperature has been calculated using Summer's relations [7]. The choice of scaling the delay time with the current sharing temperature in the peak field zone, is motivated by conservative reasons (the zones with lower fields have current sharing temperatures less sensitive to the operating current).

Table VII : Current sharing temperature Θ_g, delay time and longitudinal propagation velocity for different values of operating current. Θ_g is calculated for the peak field zone of the outer layer.

Iop/Imax	Θ_g (K)	Delay time (ms)	v_l inner layer (m/s)	v_l outer layer (m/s)
1	6.98	40	18	4.5
0.75	10.12	85	6.2	3
0.5	12.89	125	2.5	1.8

Figs. 16 and 17 display hot spot temperature and maximum voltage vs. fraction of maximum operating current. For all these cases it appears that the worst situation occurs at the maximum value of operating current. In the simulations the following values have been kept constant:

    Detection threshold voltage= 10 mV

    Dump resistor = 25 mohm
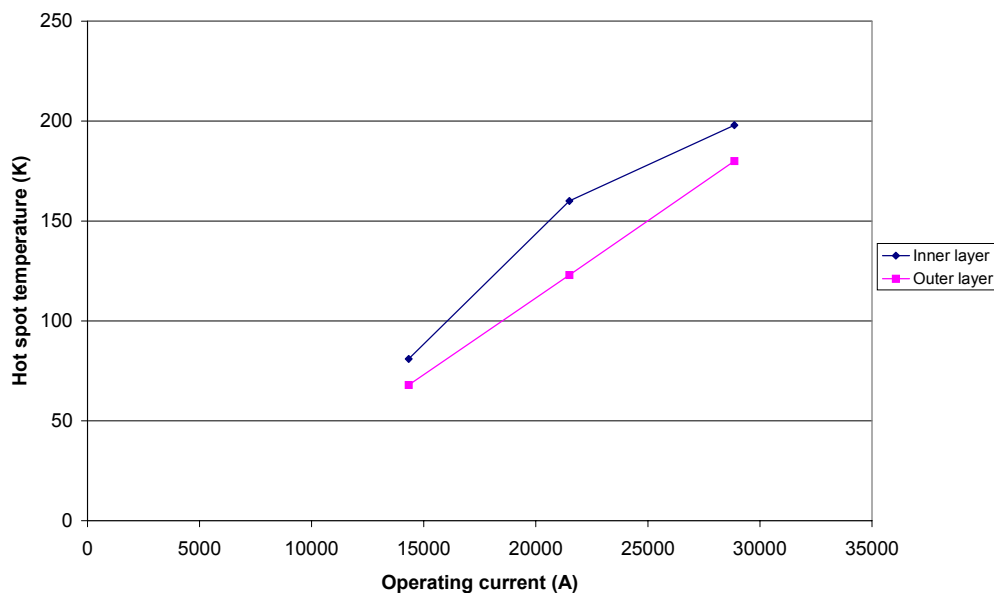
    Heaters length = 5 m

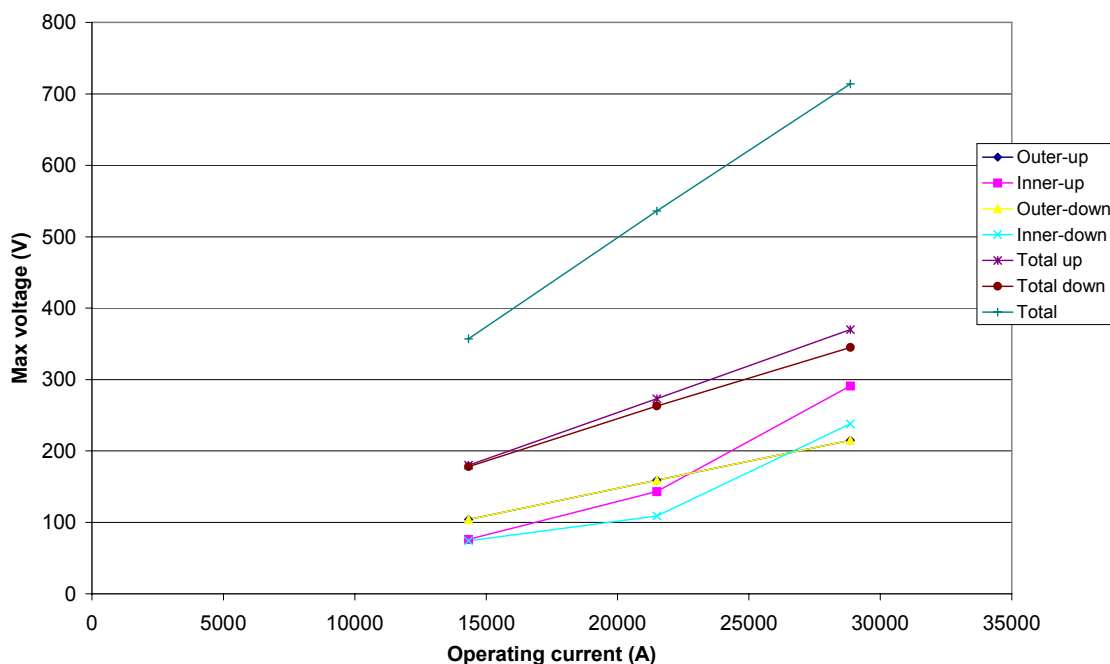Fig. 16 : Hot spot temperature in each layer vs. operating current.

Fig. 17 : Maximum voltage in each winding and in the whole magnet vs. the operating current.

2.3 10-m-long prototype: initial quench in the peak field zone

The quench study in the 10-m-long prototype has been performed considering the presence of quench heaters on the coils. As in the case of the 5-m-long prototype, the quench heaters are supposed to be glued onto the external surface of the straight sides of the outer layer. They are 5 cm high and their length has been varied in order to assess its influence on magnet protection. The quench starts in the inner layer, in the peak field zone (point D of Fig. 3) and it spreads in the entire magnet as described for the 5-m-long prototype.

Several simulations have been performed, in order to determinate the optimal value of dump resistor and the influence of the delay time, heater length and operating current on the quench development. The limit chosen for the maximum voltage in the magnet is 800 V, and the maximum allowable temperature is 300 K, like in previous cases. The paragraph 2.4 will treat a similar case but when the quench originates in the low field region. Appendix A reports the evolution of current, hot spot temperature and voltages for different values of the dump resistor.

2.3.1. Influence of dump resistor

By increasing the value of the dump resistor, the energy it dissipates will increase, so the hot spot temperature on each coil will diminish, but the total voltage will increase. This influence is well described in Figs. 18, 19 and 20, where the fractions of dissipated energy in the magnet, hot spot temperatures and maximum voltages are represented as a function of dump resistor value. In the simulations, the following parameters have been kept constant:

    Detection threshold voltage = 10 mV
    Delay time = 30 ms
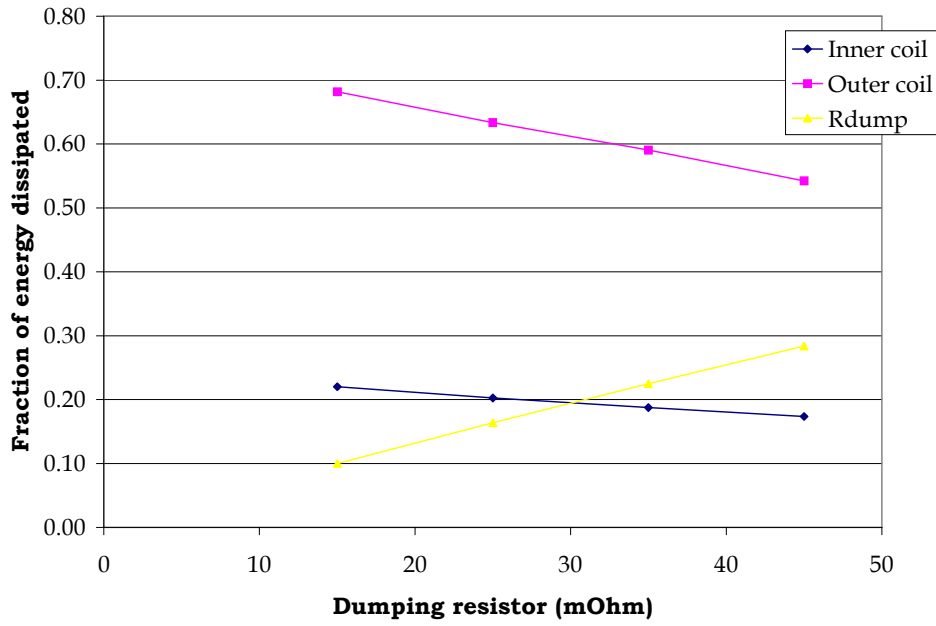   Heaters length = 10 m

Fig. 18 : Fractions of energy dissipated in each layer and in the dump resistor vs. value of dump resistor
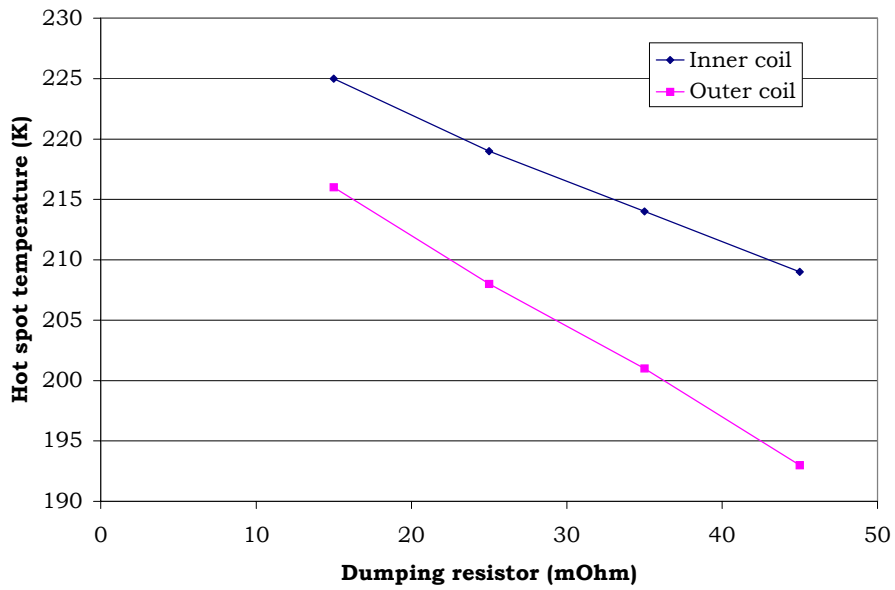

Fig. 19 : Hot spot temperature in each layer vs. value of dump resistor.
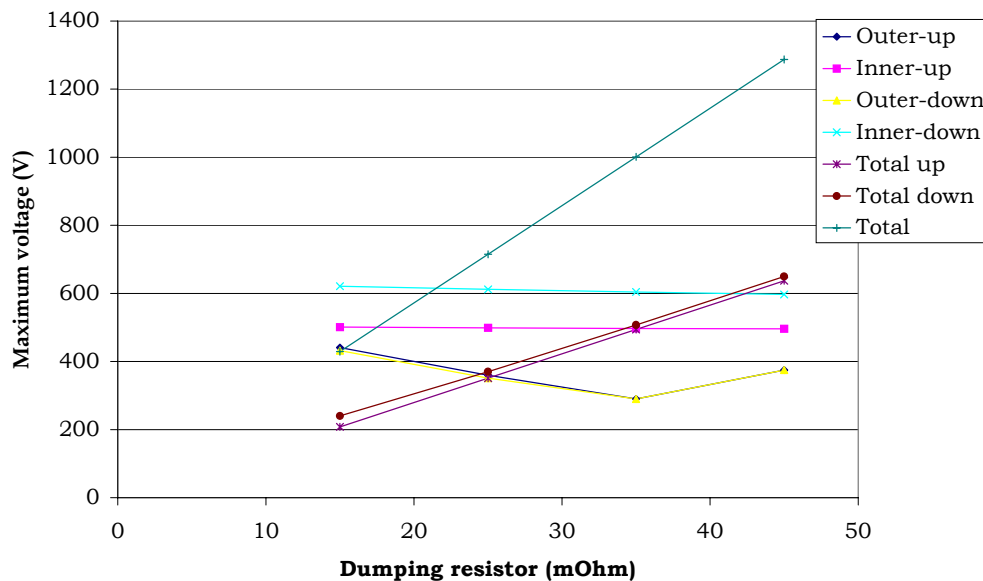
Fig. 20: Maximum voltage across each winding and across the whole magnet vs. value of dump resistor.

It appears that it is the maximum voltage across the whole magnet that limits the value of the dump resistor. In order to keep this voltage below 800 V, we need to choose a dump resistor of 25 mohm or less.

2.3.2 Influence of delay time

This delay corresponds to the time that the protection device takes to initiate extended quenches on the outer layers by means of the heaters, after the spontaneous quench is detected on the inner layer of the magnet. The longer this time, the larger the dissipated energy in the inner layer, and the greater the hot spot temperature of this layer. This behaviour can be observed in Fig. 21, where the hot spot temperature vs. delay time is represented. Fig. 22 displays maximum voltage vs. delay time. The case with a delay time of 70 ms appears to be critical: in fact the temperature is close to 300 K and the section where the quench was initiated (inner-up) reaches almost 1.000 V. For the simulation with delay time 70 ms, it has been specifically assumed a different delay time for the opening of the main switch (i.e. 40 ms), otherwise the temperature would even exceed 300 K. Consequently we can conclude that the delay time is not a critical parameter provided that it is lower than 50 ms.

Detection threshold voltage = 10 mV
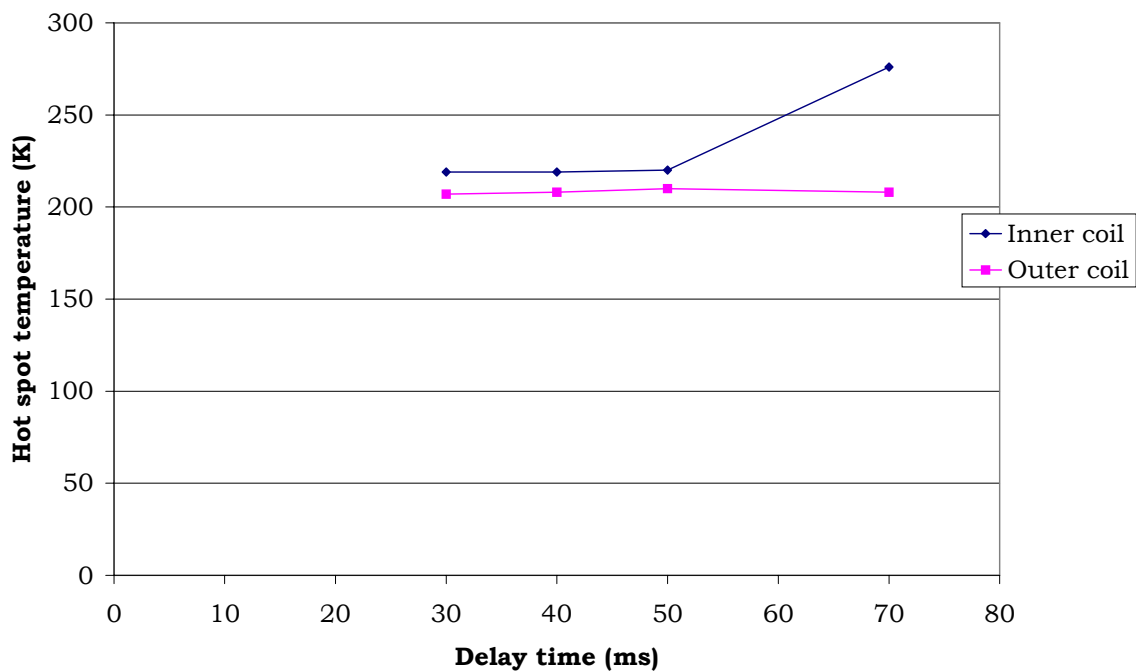Dump resistor = 25 mOhm
Heaters length = 10 m

15
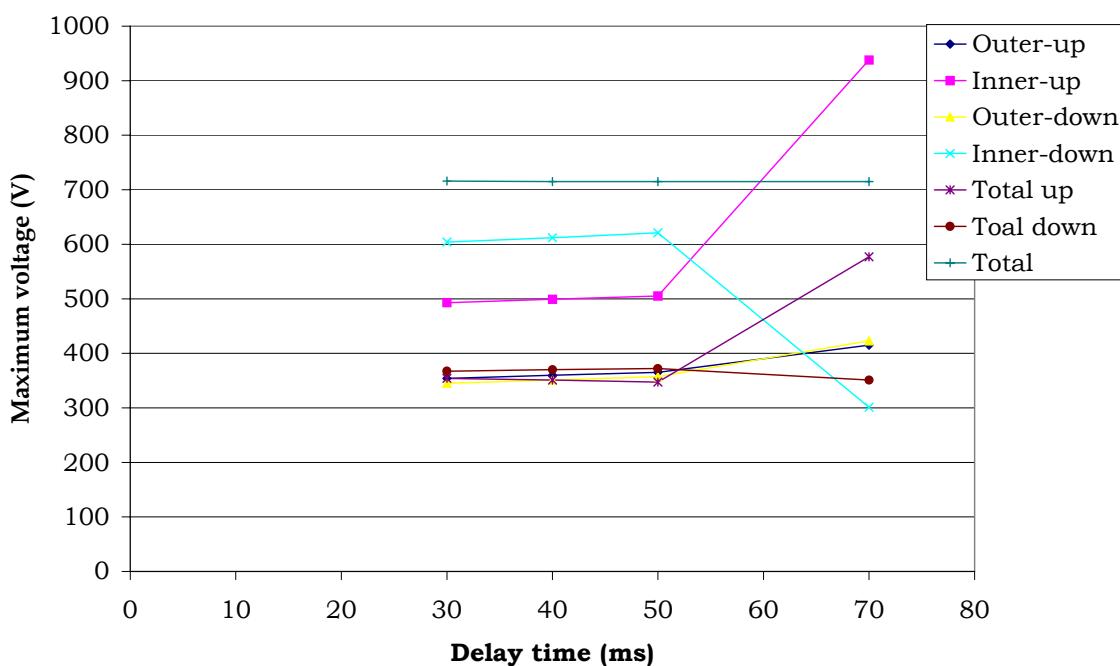
Fig. 21 : Hot spot temperature in each layer vs. delay time.

Fig. 22 : Maximum voltage in each layer and in the whole magnet vs. delay time.

2.3.3 Influence of quench-heaters length

Fig. 23 and Fig. 24 display hot spot temperature and maximum voltage vs. quench heater length. The hot spot temperature is quite sensitive to heater length: in order to keep the temperature below 250 K, it is necessary to have quench heater longer than 8.5 m. In the simulations the following values have been kept constant:

     Detection threshold voltage = 10 mV

     Dump resistor = 25 mohm

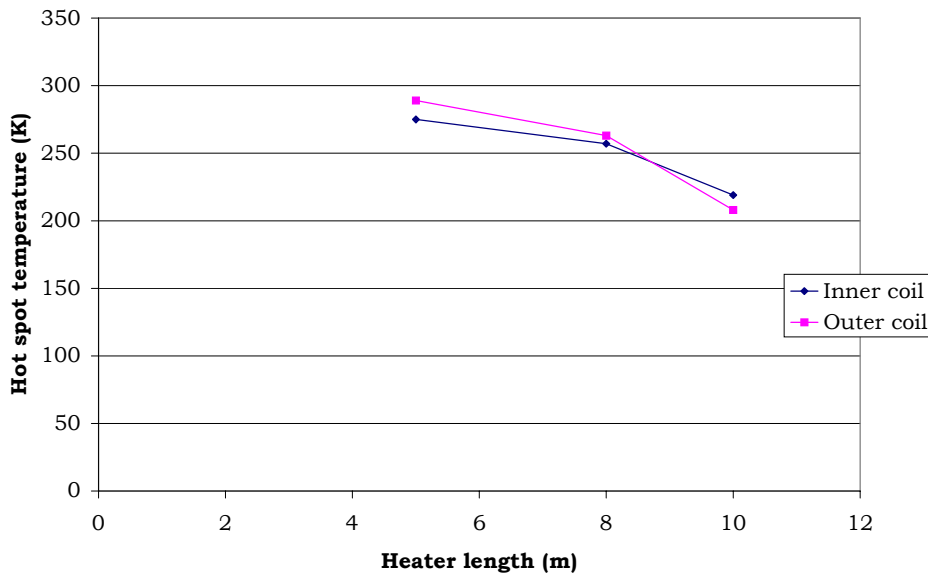   Delay time = 40 ms

16

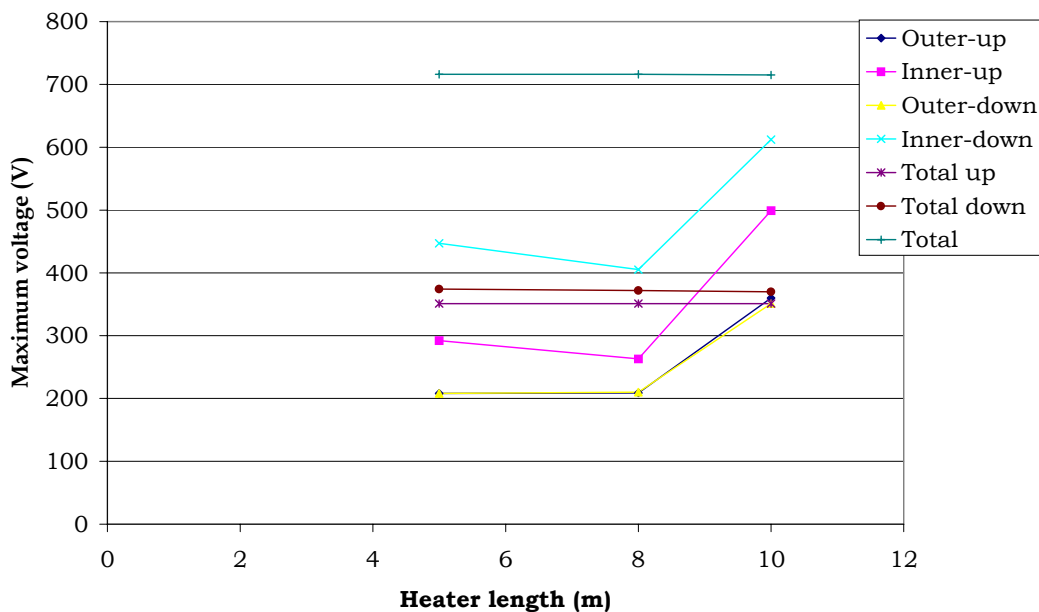Fig. 23 : Hot spot temperature in each layer vs. quench-heaters length

Fig. 24 : Maximum voltage in each layer and in the whole magnet vs. quench-heater length.

2.3.4 Influence of operating current

As explained in paragraph 2.2.4, we assume that the delay time is directly proportional to the current sharing temperature of the conductor (see Table VII).

Figs. 25 and 26 display hot spot temperature and maximum voltage vs. operating current. For all these cases it appears that the worst situation occurs at the maximum value of operating current. In the simulations the following values have been kept constant:

Detection threshold voltage = 10 mV
Dump resistor = 25 mohm
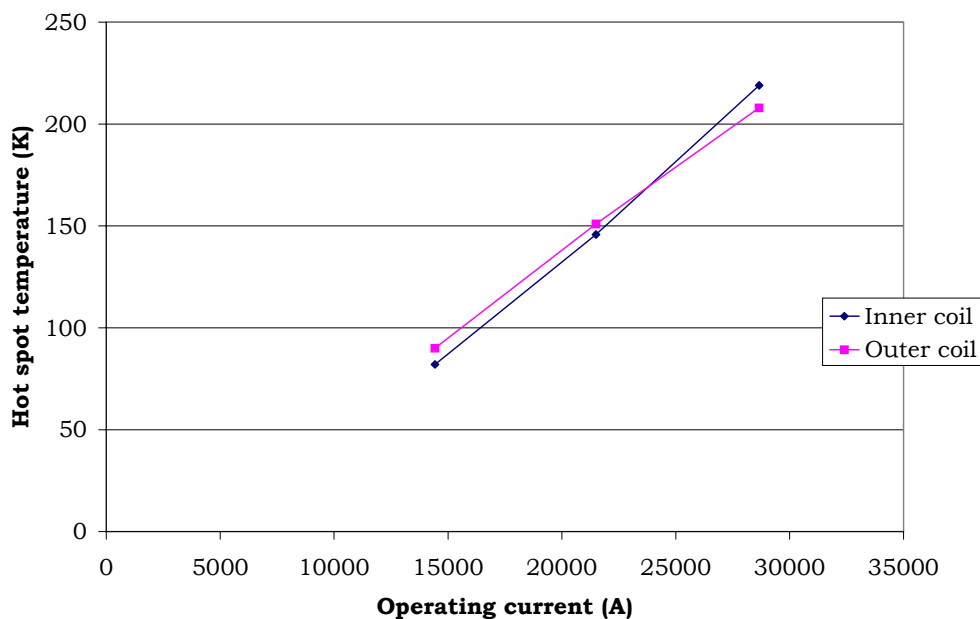Heaters length = 10 m

17

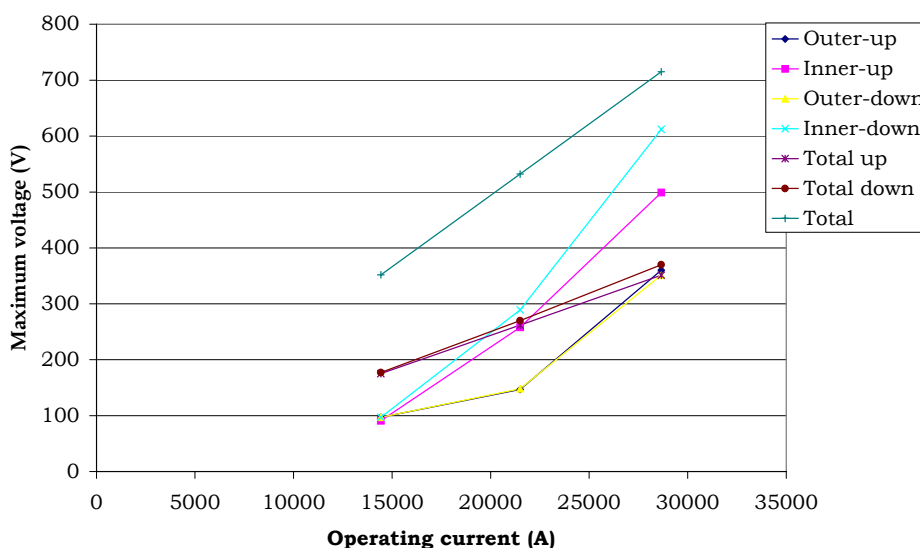Fig. 25 : Hot spot temperature in each layer vs. the operating current.

Fig. 26 : Maximum voltage in each winding and in the whole magnet vs. the operating current.

2.3.5 Influence of copper RRR

In the previous paragraphs it was assumed a constant value for the copper RRR in the conductor equal to 100. In this section we wanted to investigate the influence of the copper RRR for the protection of the magnet. Figs. 27 and 28 display hot spot temperature and maximum voltage vs. copper RRR. The following parameters have been kept constant:

    Detection threshold voltage = 10 mV
    Dump resistance = 25 mohm
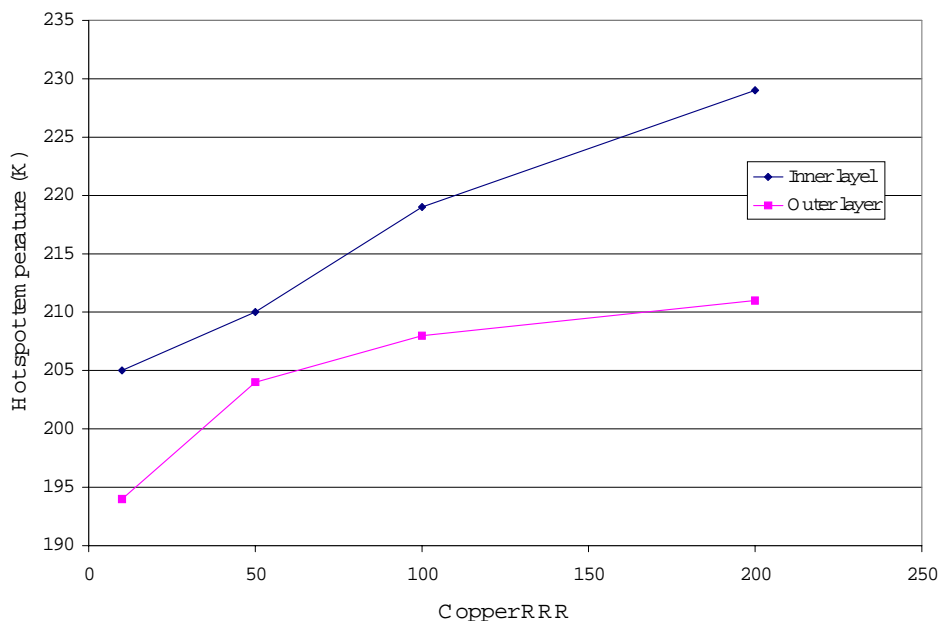   Delay time = 40 ms
    Heaters length = 10 m

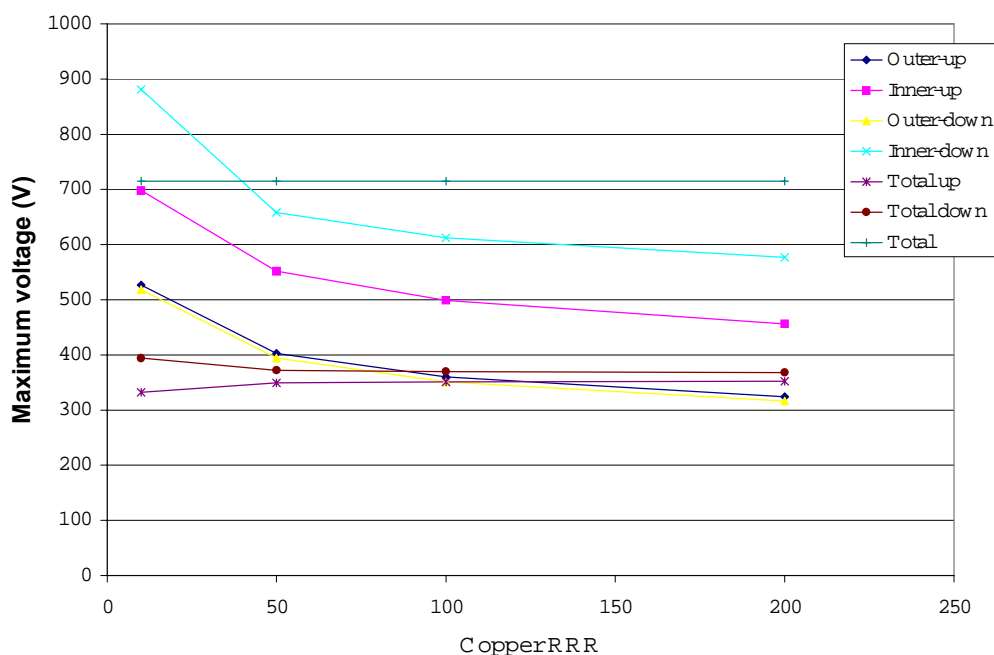Fig. 27 : Hot spot temperature in each layer vs. copper RRR.

Fig. 28 : Maximum voltage in each winding and in the whole magnet vs. copper RRR.

It can be observed that until the RRR is higher than 50, the maximum voltages can be considered below safe values, whereas at lower values the voltages increase rapidly.

2.3.6 Influence of Cu/not-Cu ratio

In the previous paragraphs it was assumed a constant value of the Cu/not-Cu ratio in the conductor equal to 1.38. In this section we wanted to investigate the influence of Cu/not-Cu ratio for the protection of the magnet. Figs. 29 and 30 display hot spot temperature and maximum voltage vs. Cu/not-Cu ratio. The following parameters have been kept constant:

Detection threshold voltage = 10 mV
Dump resistance = 25 mohm
Delay time = 40 ms
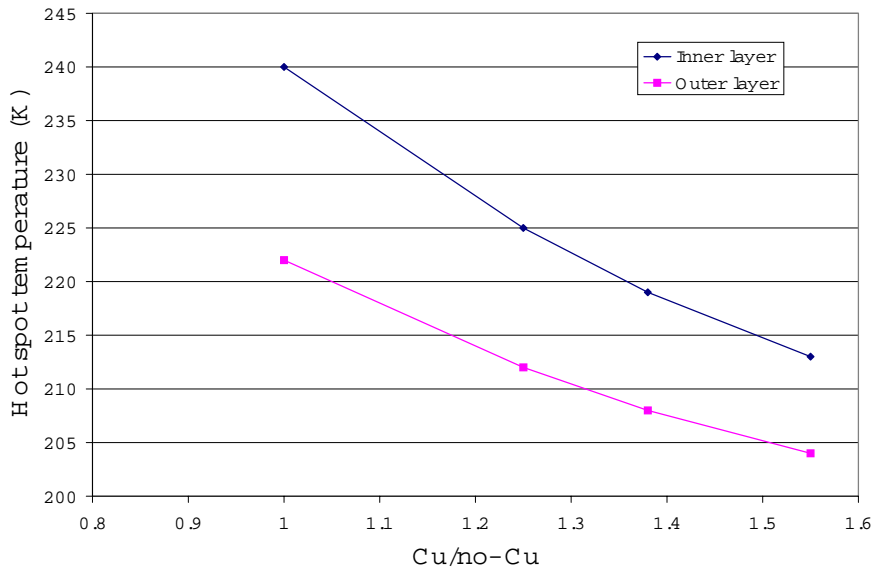Heaters length = 10 m
Cu RRR = 100

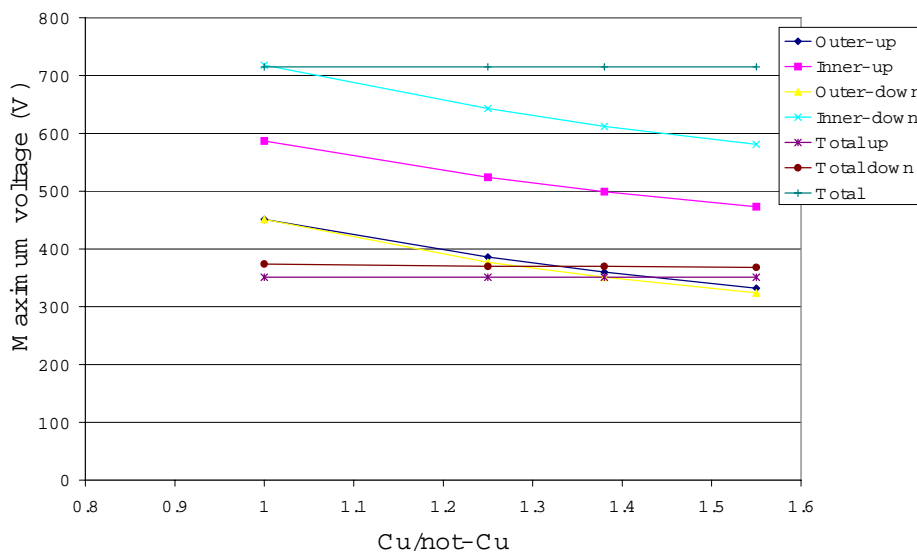Fig. 29 : Hot spot temperature in each layer vs. Cu/not-Cu ratio.

Fig. 30 : Maximum voltage in each winding and in the whole magnet vs. Cu/not-Cu ratio.

From the results we can conclude that the Cu/not-Cu ratio has significant influence on the hot spot temperature and maximum voltages, and its value should not be lower than 1.

2.4 10-m-long prototype: initial quench in the low field zone
When a quench starts in a low field region, the effects may be more dangerous because the propagation velocities are lower and, consequently, the magnetic energy is dissipated less uniformly

in the entire volume of the magnet. This can cause higher hot spot temperature and higher voltage in the coil with respect to the case where the quench originates in the peak field region.

For this reason we have simulated for the 10-m-long prototype a quench starting in the outer layer, in the external region close to the median plane where the field assumes the value of 3.7 T at the operating current, instead of 15 T in the peak field region.

In the following paragraphs we present the behaviour of the hot spot temperature and maximum voltages vs. value of the dump resistor, delay time, quench heater length and operating current.

2.4.1 Influence of dump resistor

Fig. 31 presents the influence of the dump resistor on the hot spot temperature. The maximum temperature is reached in the outer layer, where the quench starts, whereas the temperature in the inner layer is much lower than in the case where the quench originates in the inner coil (see Fig. 19). Even if the hot spot temperature is higher than the previous cases, it is well below the limit value of 300 K.

Detection threshold voltage= 10 mV
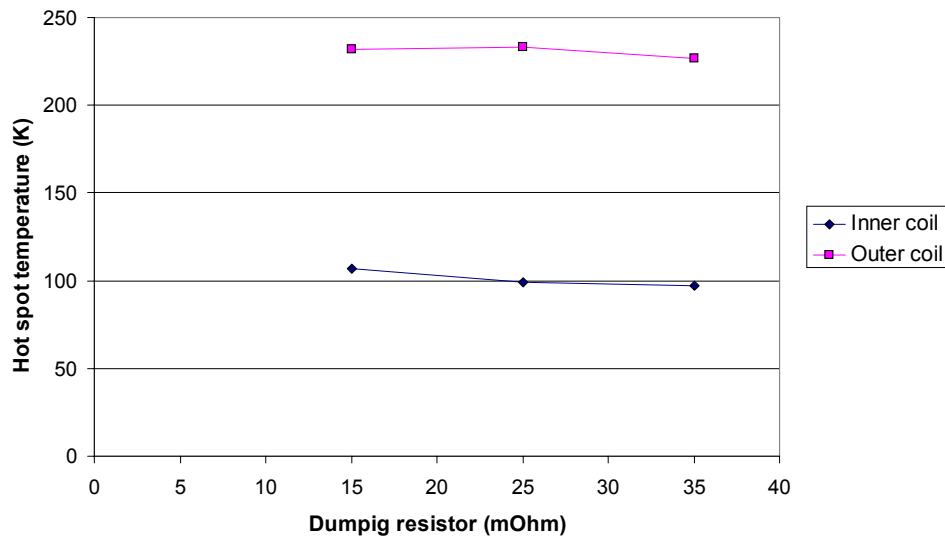Delay time = 30 ms
Heaters length = 10 m

Fig. 31 : Hot spot temperature in each layer vs. value of dump resistor.

Fig. 32 presents the maximum voltages across the various magnet sections. In this case the voltage drop in the Inner-up section is equal to the voltage drop in the Inner-down section, because the origin of the quench is the coil mid-plane and consequently it propagates symmetrically in the up and down sections. The same effect can be observed in the Outer-up and Outer-down sections.
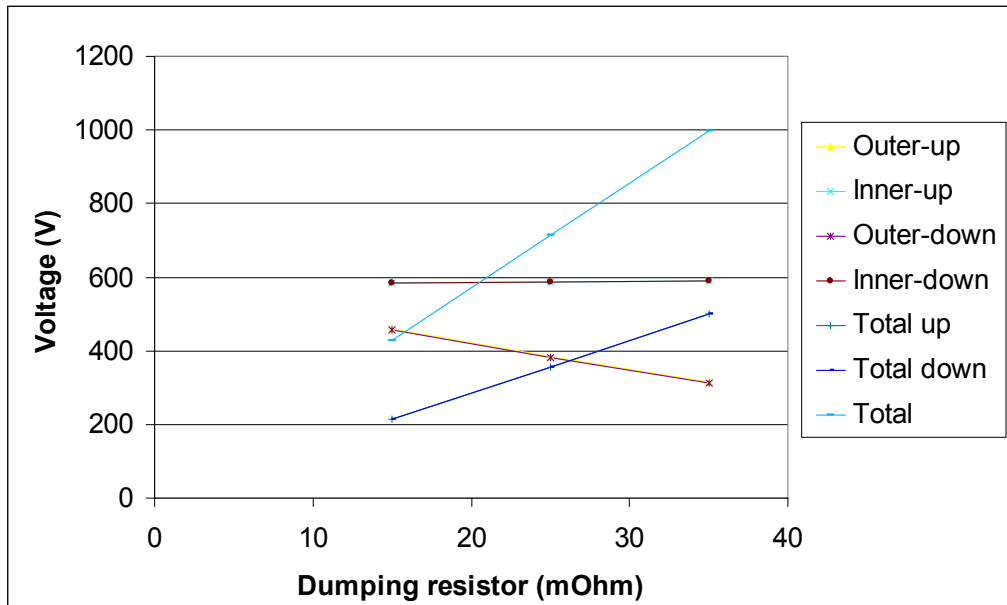
Fig. : 32 Maximum voltage across each winding and across the whole magnet vs. value of dump resistor

It appears again that it is the maximum voltage across the whole magnet that limits the value of the dump resistor. In order to keep this voltage below 800 V, we need a dump resistor of 25 mohm or less.

2.4.2 Influence of delay time

Detection threshold voltage= 10 mV
Dump resistor = 25 mohm
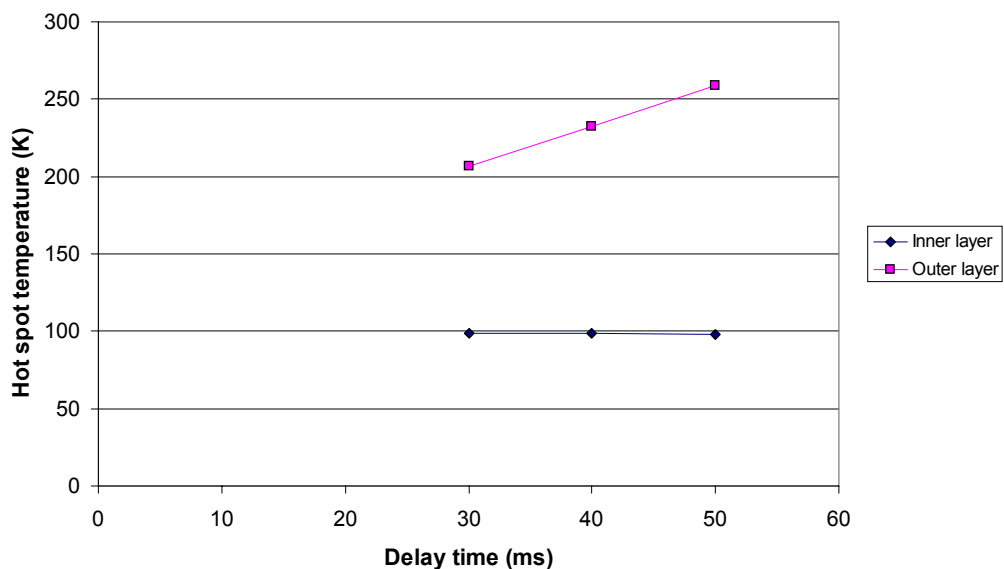Heaters length = 5 m

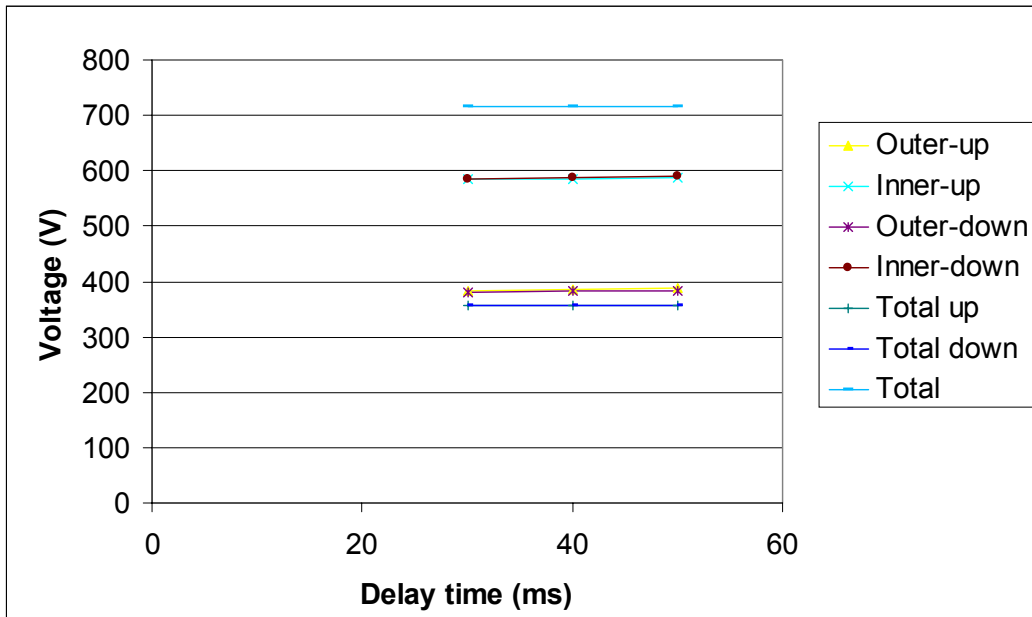Fig. 33 : Hot spot temperature in each layer vs. the delay time.

Fig. 34 : Maximum voltage in each layer and across the whole magnet vs. the delay time.

From this analysis we can conclude that the delay time is not a critical parameter for the protection of the magnet. A typical delay time for accelerator magnet of about 40 ms can be assumed to be sufficient for our purpose.

2.4.3 Influence of quench-heaters length

Fig. 35 and Fig. 36 display hot spot temperature and maximum voltage vs. quench heater length. The hot spot temperature is quite sensitive to heater length, which should be at least 7 m long. In the simulations the following values have been kept constant:

  Detection threshold voltage =10 mV
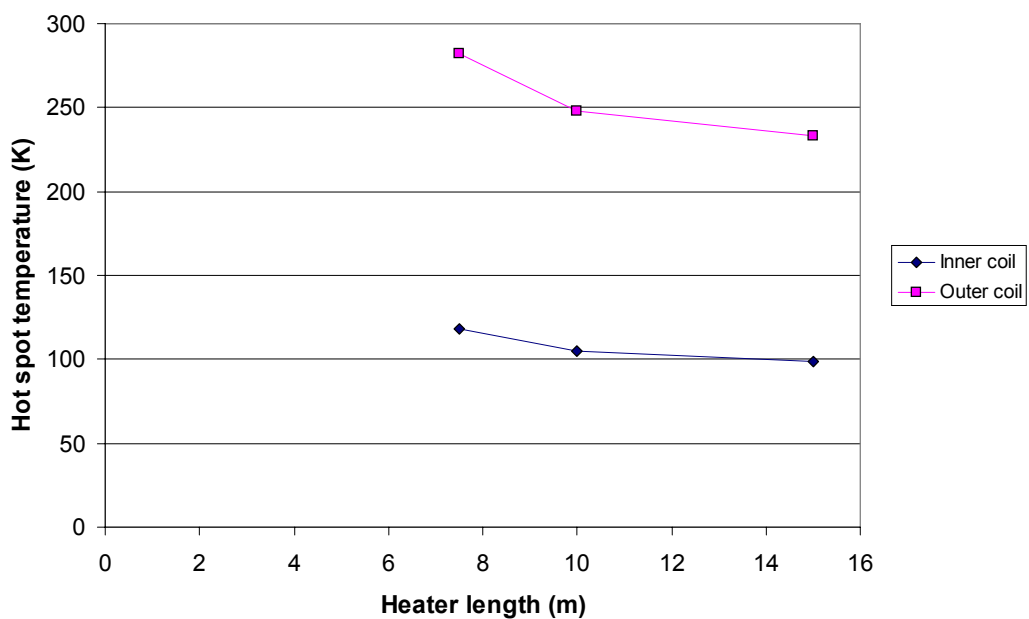 Dump resistor = 25 mOhm
  Delay time = 40 ms

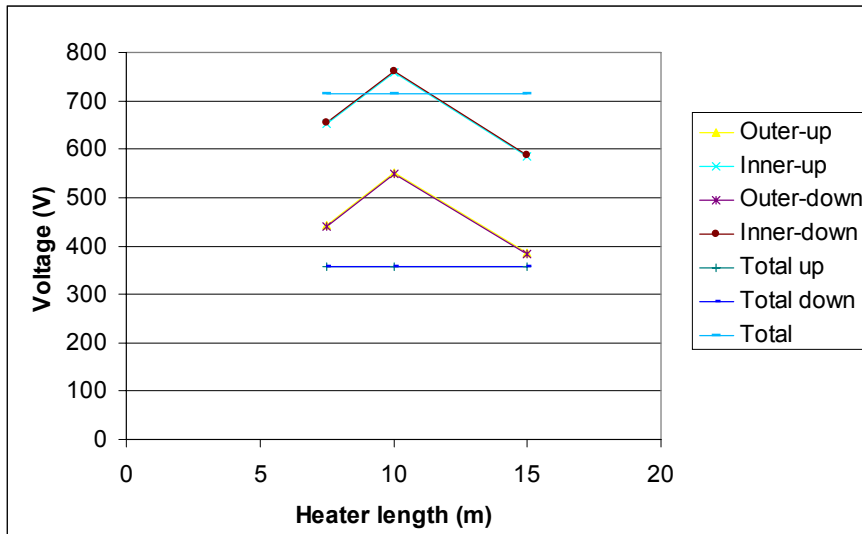Fig. 35 : Hot spot temperature in each layers vs. quench-heaters length.

Fig. 36 : Maximum voltage in each layer and in the whole magnet vs. quench-heater length.

2.4.4 Influence of operating current

Figs. 37 and 38 display hot spot temperature and maximum voltage vs. operating current. In all these cases it appears that the worst situation occurs at the maximum value of operating current. In these simulations the following values have been kept constant:

    Detection threshold voltage:=10 mV
    Dump resistor = 25 mohm
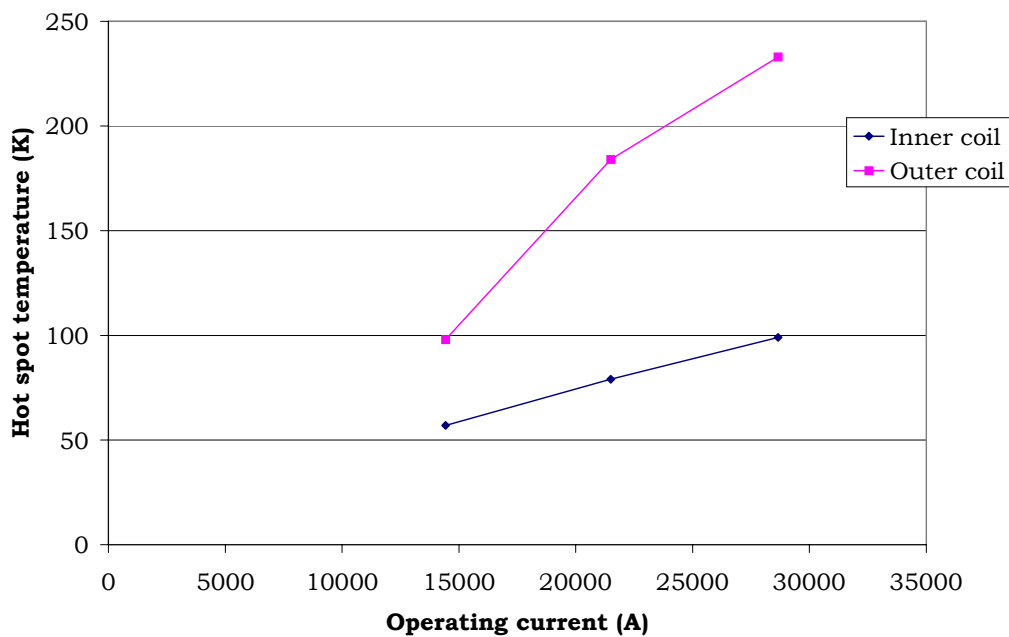   Heaters length = 5 m

Fig. 37 : Hot spot temperature in each layer vs. operating current.
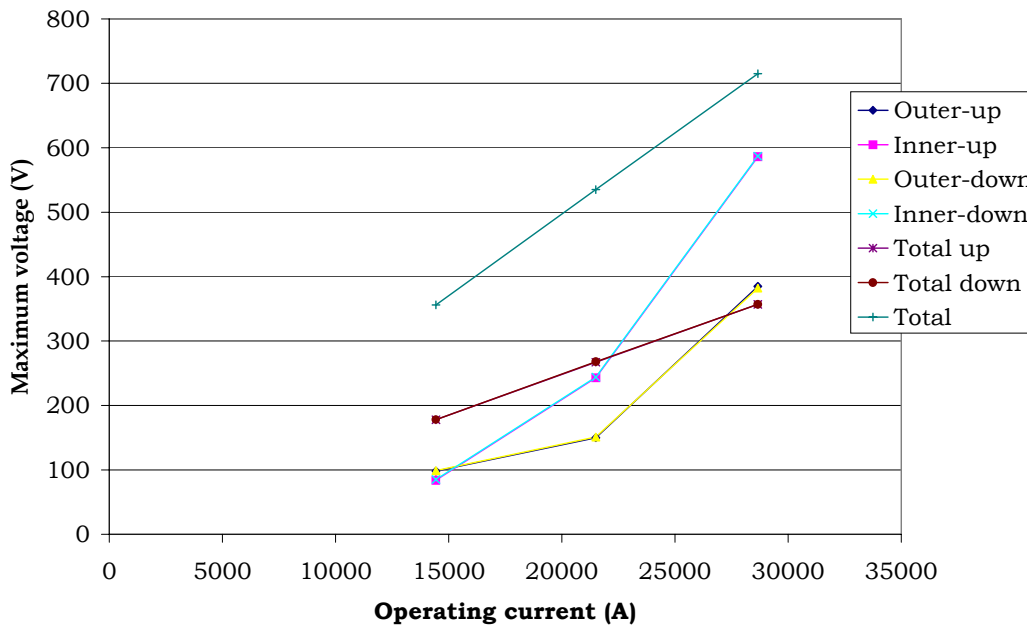
Fig. 38 : Maximum voltage in each winding and in the whole magnet vs. operating current.

3. SIMULATIONS WITH QUABER CODE

Simulations were performed also with the program QUABER [8] (Quench simulations with SABER [9]) for the three magnet prototypes of 1, 5 and 10 meters length.

In this chapter we briefly describe the simulation program (section 3.1) and we discuss the main results (sections 3.3). The simulations were performed for a spontaneous quench starting in the highest field region of the magnet and propagating along the cable and from one cable to the neighbors.
The hot spot temperature and the total voltage across the magnet were studied for several values of dump resistance, heater and switch delays and for several operating current. In Appendix B we report, for each configuration and for each prototype, plots of the current, of the hot spot temperature and of the voltages across the various magnet sections.
In section 3.4 the case of a quench starting in a low field region is also illustrated.

QUABER includes a subroutine to calculate quench velocities for NbTi cables, based on analytical formulas [4] in adiabatic approximation, which gives only an estimation of the longitudinal and transversal velocities. For this reason, simulations of the quench velocity in Nb_3Sn cables were performed with the program SPQR (Simulation Program for Quench Research). The results of these simulations are reported in section 3.2, and they were used as an input to QUABER.

The results obtained with QUABER were cross checked with simulations performed under the same assumptions with QLASA. For both programs the same libraries of physical properties, (resistivity, thermal conductivity and specific heat) of the conductor components (Nb_3Sn, Sn, Cu, Ta, CuSn) and of the insulation layer (G10) were used. In section 4 a comparison of the hot spot temperature and of the total voltage calculated with the two programs is reported.

3.1 The numerical code QUABER.

QUABER is a collection of scripts written in the language MAST. QUABER was written to study the quench propagation and the protection system of the LHC magnets which are based on NbTi cables. The scripts run on a commercial analysis interface called SABER. SABER is an analog System Analysis Program (SAP) designed to solve electrical circuits and it provides a list of accessible templates included into a standard library. QUABER must be provided with a list of inputs such as cable characteristics, material properties, magnet geometry and magnetic field map.

The QUABER scripts were written to integrate thermal and electrical processes related to the propagation of a quench in a superconducting magnet. The extension of the normal zone, its resistance and temperature are calculated at each time step. The quench resistance is a non-linear function of temperature and magnetic field. Both temperature and magnetic field are time dependent variables. The simulator (SABER) solves the electric circuit taking into account the value of the quench resistance at each time step.

To be used for the NED dipole prototype the QUABER scripts had to be adapted to Nb$_3$Sn cables taking into account the physical properties of the cable components (superconductor, matrix and insulation). The modifications were included into the scripts using data from the QLASA libraries to make possible a direct comparison between the results obtained with the two programs.

The material properties of the conductor as function of the temperature and of the magnetic field are used to calculate the MIITs number (the integral in time of the current squared). Knowing the MIITs number at time t, it is possible to calculate the temperature T in the conductor by solving the heat balance equation:

$$ A_{Cu} \cdot A_{total} \cdot \int_{Tbath}^{T} \frac{C(T)}{\rho_{Cu}(B,T,RRR)} \cdot dT = \int_{t_q}^{t} I^2(t) \cdot dt $$

where A_{Cu} and A_{total} are the copper section and the total section of the conductor respectively. $C(T)$ is the average specific heat of the conductor (of the superconductor and of the copper). $\rho_{Cu}(B,T,RRR)$ is the copper resistivity for a given magnetic field, temperature and Residual Resistivity Ratio.

The user gives the position where the quench originates. At time equals zero the transition starts to propagate with a longitudinal velocity along the cable and a transverse velocity to the neighboring cables. The initial velocities are given as input and are corrected according to the current level by an empirical relation between current and velocity [8].

$$ v = v_0 \cdot \frac{I(t)}{I_0} \cdot \left(1 + a \cdot \frac{I(t)}{I_0} \right) \cdot \frac{1}{1+a} $$

where a is a parameter determined experimentally which varies between 0.2 and 0.5. v_0 and I_0 are the initial velocity and the initial current. The simulations reported here were made using a parameter a with a value of 0.2, while the initial velocities were independently calculated with the programs QLASA and SPQR and included as input values in QUABER.

In the next section simulations of quench velocities made with SPQR are reported. The longitudinal velocities calculated with SPQR are in good agreement with the velocities calculated with QLASA except for the value at maximum current. At maximum current the longitudinal velocity calculated with QLASA is a factor 3 smaller than the value calculated with SPQR. The discrepancy is related

to the different approach used in the two programs to model the quench propagation and to calculate the quench velocity.

The simulations made with QUABER and discussed in section 4 use the velocity calculated with QLASA. This choice is justified to simulate the worst scenario for quench propagation and to enable a direct comparison of the results obtained with QUABER and QLASA.

3.2 Quench velocities calculated with SPQR.

The program SPQR was developed to compute the quench process in superconducting magnets and busbars. The model approximates the heat balance equation with the finite difference method including the temperature dependence of the material parameters. SPQR allows the simulation of the longitudinal and transverse quench propagation, heat transfer into a helium bath through an insulation layer, forced quenches with heaters and the impact of eddy currents. For our purpose SPQR was mainly used to calculate the initial longitudinal and transverse velocities which were then included as input parameters in QUABER. Like QUABER, SPQR was written for the NbTi LHC magnets, and therefore the physical properties of the cable components were modified in the program to adapt it to Nb_3Sn magnets. In this section we limit our discussion to the main results of the simulations, a detailed description of the program can be found in [10].

An example of the temperature profile evolution in a Nb_3Sn cable is shown in Fig. 39. The simulation was made for a 1 m long cable and the time step between two curves is 0.2 ms.
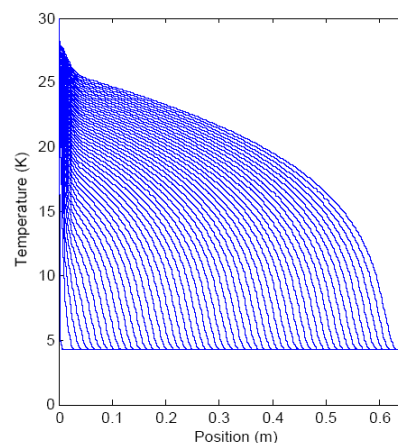

Fig. 39 Temperature profile along a 1-m-long Nb_3Sn cable. The time step between two curves is 0.2 ms.

The quench produced in a cable can propagate through the insulation layer to the neighboring cables. The cables are insulated with a 0.2 mm thick G10 layer. An example of the transversal quench propagation is shown in Fig. 40. Here the temperature profiles of two neighboring cables are plotted. The quench starts in the cable on the left and propagates to the cable on the right through the insulation.
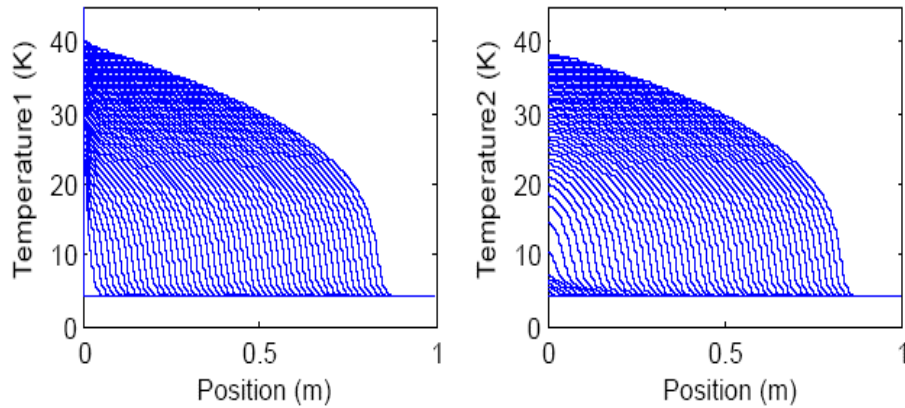
Fig. 40 Temperature profile in two adjacent, 1-m-long Nb$_3$Sn cables. The quench starts in the cable on the left and propagates through 0.4 mm of insulation (G10) to cable 2. The time step between two curves is 0.2 ms.

The simulations were carried out to calculate the longitudinal velocity (vl) and the transverse propagation time (ttd, turn to turn delay) at several operating current and magnetic field values for both the inner and outer layer. The ttd is the time elapsed since the beginning of a quench in cable 1 until the temperature in cable 2 rises above the current sharing temperature .
The results of the simulations with SPQR are reported in Table VIII with also the longitudinal velocity values calculated with QLASA.

Table VIII: Longitudinal velocity and turn-to-turn delay calculated with SPQR for several values of operating current and magnetic field. The longitudinal velocities calculated with QLASA are also reported. Tc is the current sharing temperature.

Inner layer	I(A)	Bmax(T)	Tc (K)	vl(m/s) (QLASA)	vl(m/s) (SPQR)	ttd (ms) (SPQR)
	14330	7.5	11.98	2.5	3.3	52
	21495	11.25	8.56	6.2	8.6	12
	28660	15	4.32	18	61	0.2

Outer layer	I(A)	Bmax(T)	Tc (K)	vl(m/s) (QLASA)	vl(m/s) (SPQR)	ttd (ms) (SPQR)
	14330	6.16	12.89	1.8	1.8	71
	21495	9.24	10.12	3	5.3	21
	28660	12.32	6.89	4.5	16.7	4.7

At maximum current the longitudinal velocity calculated with QLASA is a factor 3 smaller than the value calculated with SPQR for both the inner and outer layer. This discrepancy is probably due to the fact that, the higher the operating current, the closer the critical temperature to the bath temperature. In SPQR the velocity exponentially diverges as the critical temperature approaches the thermal bath. This is related to the way the program models the quench propagation with temperature.

3.3 Simulation results with QUABER
In QUABER the magnet was schematically represented as composed of two layers and seven blocks. The copper spacers were not included in the simulation design because their contribution in terms of propagation delay of the quench from one block to the neighbor block is negligible compared to the transverse velocity of the quench through the insulation layer of G10.

The simulations were performed by assigning to the cables of a same block the maximum field value in that block. No significant differences in terms of hot spot temperature and voltage across the sectors were observed when using a more detailed field map.

We report here the results of simulations made using several values of dump resistance (section 3.3.1), switch and heater delays (section 3.3.2) and operating current (section 3.3.3). For each parametric configuration the simulations were performed on 1, 5 and 10 meter long prototypes.

3.3.1 Dump resistor

Simulations were performed with three different values of the dumping resistances: 15 mΩ, 25 mΩ and 35 mΩ. The magnet inner and outer layers are considered as composed of four sectors: inner upper, inner lower, outer upper and outer lower. The hot spot temperature and the total voltage across the magnet and across each of the four sectors were calculated.

In Table IX we report the values of these parameters as well as the longitudinal velocity and the turn-to-turn delay used in the simulations. The values of the hot spot temperature, the total voltage and the voltage across the four sectors for a magnet of 1, 5 and 10 meters length are reported.

A natural quench starts in the inner layer upper sector (block 4, cable 19), it propagates with a longitudinal velocity of 18 m/s along the cable and from one cable to the neighbors with a delay time of 5 ms. The operating current is 28660 A.

After a delay time of 40 ms the switch opens and the heaters are effective, and consequently a quench is produced in every cable of the outer layer.

At the moment the switch is open, part of the power starts to dissipate also in the dump resistor. The current decreases with a time constant $\tau = LR_{dump}$, where L is the magnet inductance, and the voltage across the four sectors abruptly increases (in absolute value) due to the current change.

Table IX: Hot spot temperatures, total voltages and voltages across the four sectors of a 1-m, 5-m and 10-m long magnet, as computed with QUABER as function of dump resistor.

Magnet length (m)	Current (A)	Rdump (mOhm)	Delay (ms)	vl (m/s)	ttd (ms)	T hot spot (K)	V total (V)	V inner up (V)	V inner down (V)	V outer up (V)	V outer down (V)
1	28660	15	40	18	5	117.1	429.4	83.3	85.5	130.3	130.3
1	28660	25	40	18	5	86.2	713.3	136.2	138.4	219.4	219.4
1	28660	35	40	18	5	73.4	995.9	188.8	191.0	308.1	308.1
5	28660	15	40	18	5	238.1	430.6	199.2	277.9	111.8	111.8
5	28660	25	40	18	5	210.7	716.6	202.4	252.2	199.7	199.7
5	28660	35	40	18	5	186.3	1002.4	211.6	240.4	289.4	289.4
10	28660	15	40	18	5	272.5	430.8	490.1	609.8	421.4	421.4
10	28660	25	40	18	5	255.3	717.1	473.8	571.0	319.2	319.2
10	28660	35	40	18	5	239.1	1003.2	459.8	537.5	263.8	263.8

The current decay, the hot spot temperature and the total voltage are shown in Fig. 41 for the case of a 5-m-long magnet. The hot spot temperature is always less than 240 K, while to keep the total voltage below 800 V it is necessary to reduce the dump resistance to 25 mΩ.

The voltage across each sector of the windings was also studied. Fig. 42 shows the trend of the four voltages (inner/outer - upper/lower) for a 5-m-long magnet. In Appendix B similar plots are presented for 1-m and 5-m long magnets.
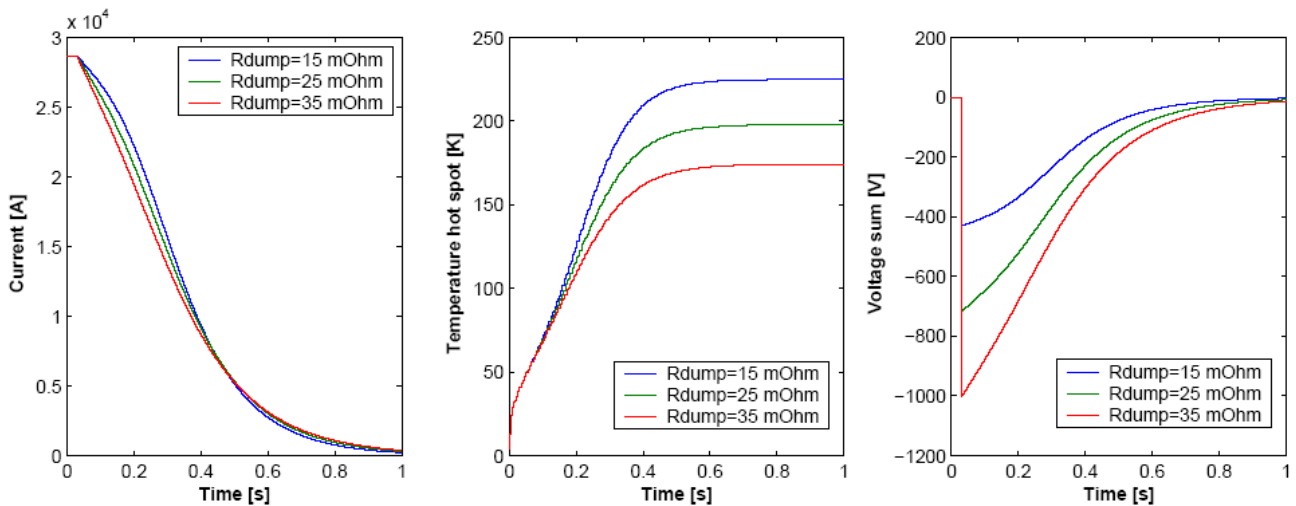
Fig. 41. Current decay, hot spot temperature and total voltage for a 5-m-long magnet.

The voltage across each sector is obtained by the balance between the inductive and resistive contribution to the signal. For the outer layer the voltage is dominated by the fast increase of the resistive zone due to the extended quench induced by the heaters over the complete surface of the outer layer. The voltage in the outer layer quickly reduces (in absolute value) to become positive when the resistive contribution to the voltage compensates and overcomes the inductive contribution.

The growth of the resistive zone in the inner layer is much slower than in the outer layer because it is related only to the propagation of the natural quench from its origin point. The voltage across the inner sectors continues to increase (in absolute value) until the normal zone has extended enough for the resistive contribution to predominate the inductive contribution.
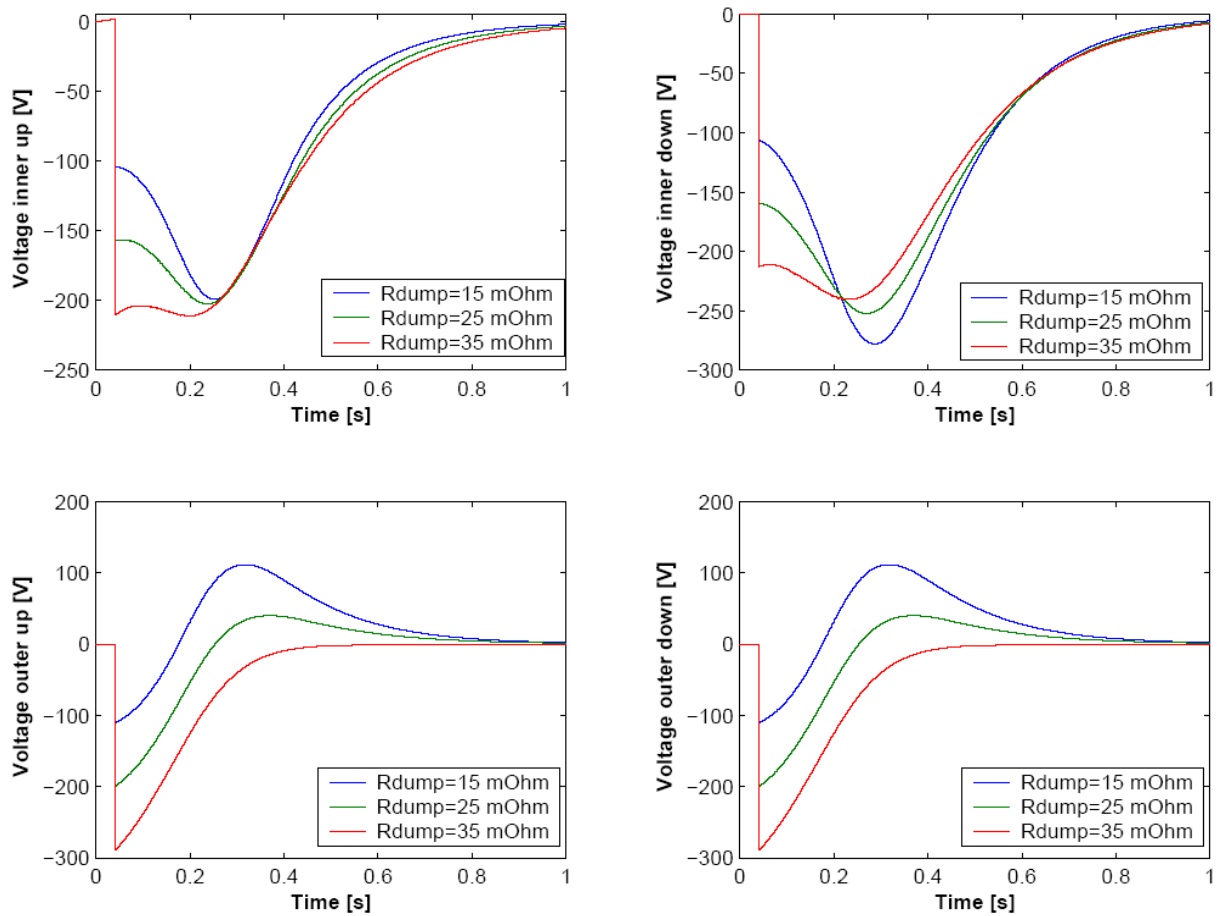
Fig. 42. Voltage across each of the four sectors of the windings for a 5-m-long magnet.

3.3.2 Heaters and switch delay

Simulations were made with a heater and a switch delay of 30, 40 and 50 ms. The delay time corresponds to the time elapsed from the beginning of a natural quench to the moment the switch is opened and the heaters are fired. For the heaters this delay time includes the time elapsed between the activation of the heaters and the appearance of a quench in the outer layer.

The results of the simulations are summarized in Table X where are reported the hot spot temperature and the voltage for the 1-m, 5-m and 10-m-long prototypes. The operating current is 28660 A and the dump resistance 25 mΩ. The longer the delay, the higher the hot spot temperature, because longer time is given to the quench to propagate at the maximum current and because for longer time the power is dissipated only in the localized resistive zone.

Table X The delay time is 30, 40 and 50 ms. Hot spot temperatures, total voltages and voltages across the four sectors for a 1-m, 5-m and 10-m-long magnet, as computed with QUABER as function of delay time

Magnet length (m)	Current (A)	Rdump (mOhm)	Delay (ms)	vl (m/s)	ttd (ms)	T hot spot (K)	V total (V)	V inner up (V)	V inner down (V)	V outer up (V)	V outer down (V)
1	28660	25	30	18	5	80.1	717.6	137.0	138.2	225.5	225.5
1	28660	25	40	18	5	86.2	713.3	136.2	138.4	219.4	219.4
1	28660	25	50	18	5	92.9	713.1	135.1	138.6	219.7	219.7
5	28660	25	30	18	5	195.7	717.6	211.7	252.3	225.6	225.6
5	28660	25	40	18	5	210.7	716.6	202.4	252.2	199.7	199.7
5	28660	25	50	18	5	226.5	716.6	191.6	252.3	200.1	200.1
10	28660	25	30	18	5	236.4	717.1	491.6	569.1	328.7	328.7
10	28660	25	40	18	5	255.3	717.1	473.8	571.0	319.2	319.2
10	28660	25	50	18	5	275.5	717.1	452.2	572.7	307.5	307.5

.

The current decay and the total voltage do not change significantly because they are mostly sensitive to the operating current and to the dump resistance values that are constant in these simulations. No significant differences are also observed for the voltages across the four sectors. In Appendix B the plots for the three prototypes can be found.

3.3.3 Operating current

The longitudinal and transverse quench velocities depend on the operating current. For a low current value, the quench propagation is slower. At low operating current it is therefore possible to extend the switch and heaters delay time. In Table XI are reported the values used for the current, the longitudinal velocity and the turn to turn delay. The delay time was linearly scaled with the sharing temperature. The dump resistance was set to 25 mΩ.

Table XI: Hot spot temperatures, total voltages and voltages across the four sectors of a 1-m, 5-m and 10-m-long magnet, as computed with QUABER as a function of operating current.

Magnet length (m)	Current (A)	Rdump (mOhm)	Delay (ms)	vl (m/s)	ttd (ms)	T hot spot (K)	V total (V)	V inner up (V)	V inner down (V)	V outer up (V)	V outer down (V)
1	14330	25	125	2.5	52	44.1	358.8	68.6	68.7	110.8	110.8
1	21495	25	85	6.2	12	65.8	535.0	102.2	103.1	164.8	164.8
1	28860	25	40	18	5	86.2	713.3	136.2	138.4	219.4	219.4
5	14330	25	125	2.5	52	71.4	358.8	76.1	76.2	103.3	103.3
5	21495	25	85	6.2	12	145.8	537.5	116.0	117.5	152.3	152.3
5	28860	25	40	18	5	213.4	716.6	201.8	248.2	199.7	199.7
10	14330	25	125	2.5	52	84.5	358.8	85.4	85.5	93.9	93.9
10	21495	25	85	6.2	12	182.2	537.8	236.0	252.9	135.7	135.7
10	28860	25	40	18	5	255.3	717.1	473.8	571.0	319.2	319.2

For every parametric configuration and for every magnet prototype the temperature is always less than 300 K and the total voltage is below 800 V. In Appendix B the current and voltage plots for the three prototypes are reported.

3.4 Quench in low field region

A quench occurs most likely in the region of the windings where the field is the highest. If a quench starts in a region where the magnetic field is low the quench propagates with a smaller velocity than when it is produced in a high field region. In a low field region the hot spot temperature is higher because the quench propagation is slower and the quench remains localized for a longer time in a small area.

Simulations of a quench starting in the outer layer, block 5, cable 20, where the magnetic field is the lowest, were performed with QUABER. In this configuration the hot spot temperature is lower than in the case of a quench starting in the inner layer (high field). The reason is that the outer layer is surrounded by heaters which are activated 40 ms after the quench starts. The heaters produce a quench in every cable of the outer layer and the normal zone is widely extended. The hot spot temperature is lower than when the quench starts in the inner layer (high field) where the diffusion of the normal zone is related only to the propagation of the initial, spontaneous, quench.

A comparison between the two configurations (quench in a low field region and quench in a high field region) for a 5-m-long magnet is shown in Fig. 43 and Fig. 44. The total voltage is the same in both configurations, while the hot spot temperatures differ of 60 K. The operating current is 28.660 A and the dump resistance 25 mΩ.
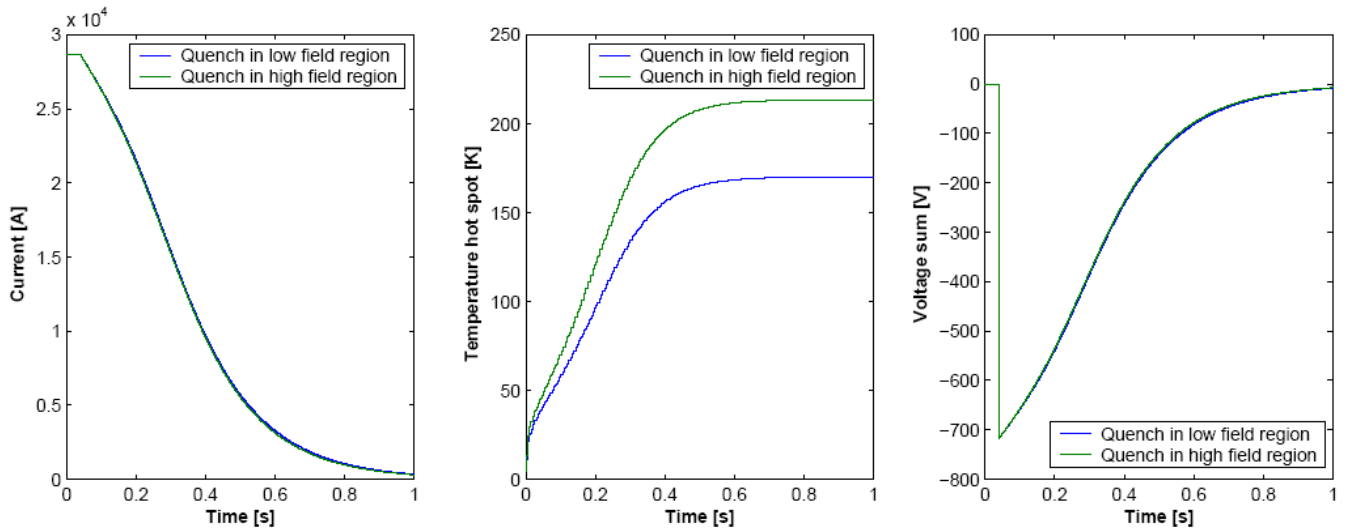
Fig. 43 Current decay, hot spot temperature and total voltage for a quench starting in a low and a high field region. The magnet is 5 meters long.
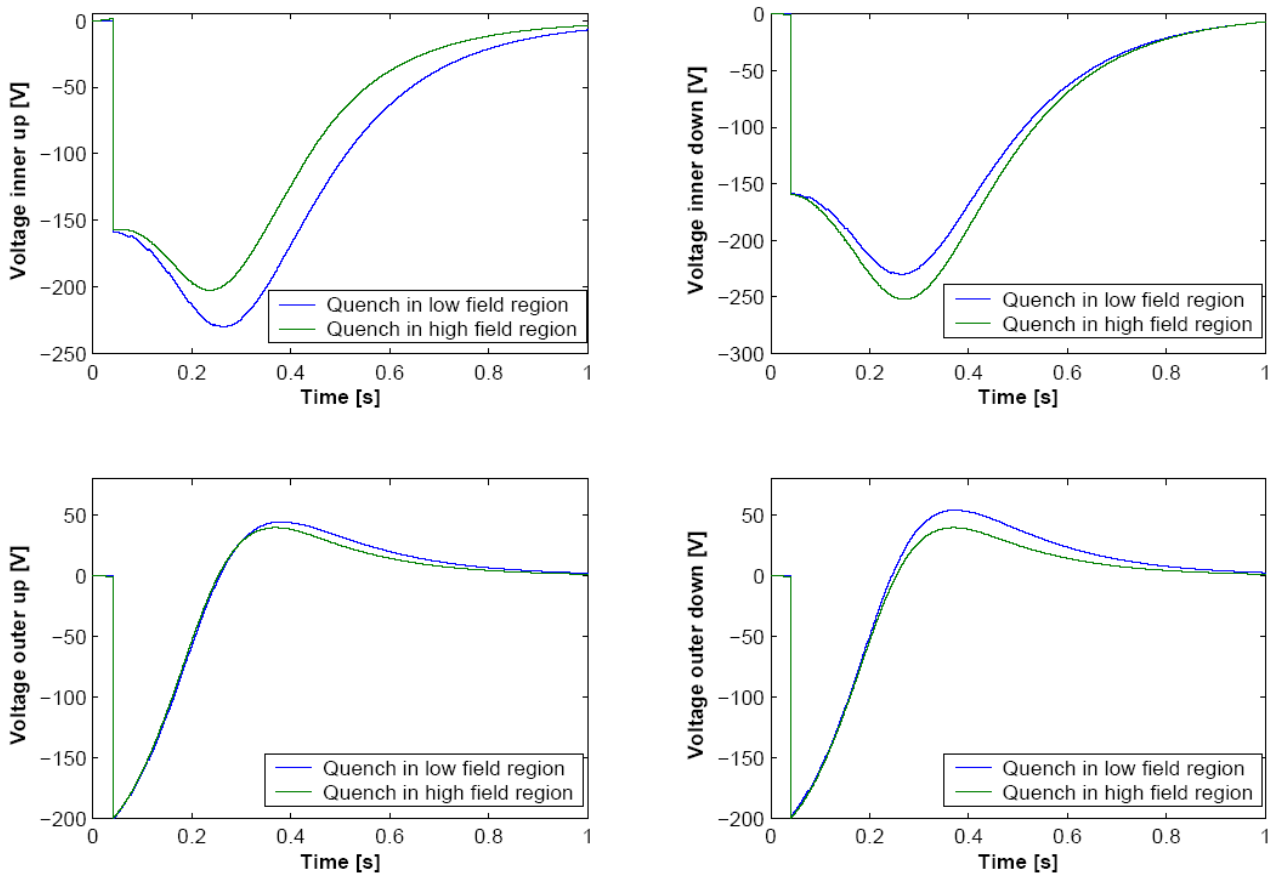

Fig. 44 Voltage across each of the four sectors of the windings for a quench starting in a low and in a high field region. The magnet is 5 meters long.

The voltages across the up and down sectors of the inner layer show some differences between the two configurations. When a quench starts in the outer layer (low field region) it propagates from this layer symmetrically to the inner up and to the inner down sectors and the voltage across them (blue line) are identical. When the quench starts in the inner layer (high field region) it propagates

33

from the inner up to the inner down producing a resistive contribution to the voltage higher in the inner up than in the inner down and therefore a smaller voltage (in absolute value, green line) in the inner up than in the inner down.

The voltages across the up and down sectors of the outer layer are instead very similar for both configurations. In the outer layer the quench propagation is controlled by the heaters and the voltage is nearly unchanged whether there is a natural quench starting in this layer or not.

4.   COMPARISON RESULTS FROM QLASA AND QUABER

The simulations performed with QLASA (section 2) were compared with simulations made with the program QUABER (section 3) in similar conditions.

The hot spot temperature and the total voltage for the 1-m and 5-m long magnets are shown in Fig. 45, whereas Fig. 46 reports the case 10-m-long.
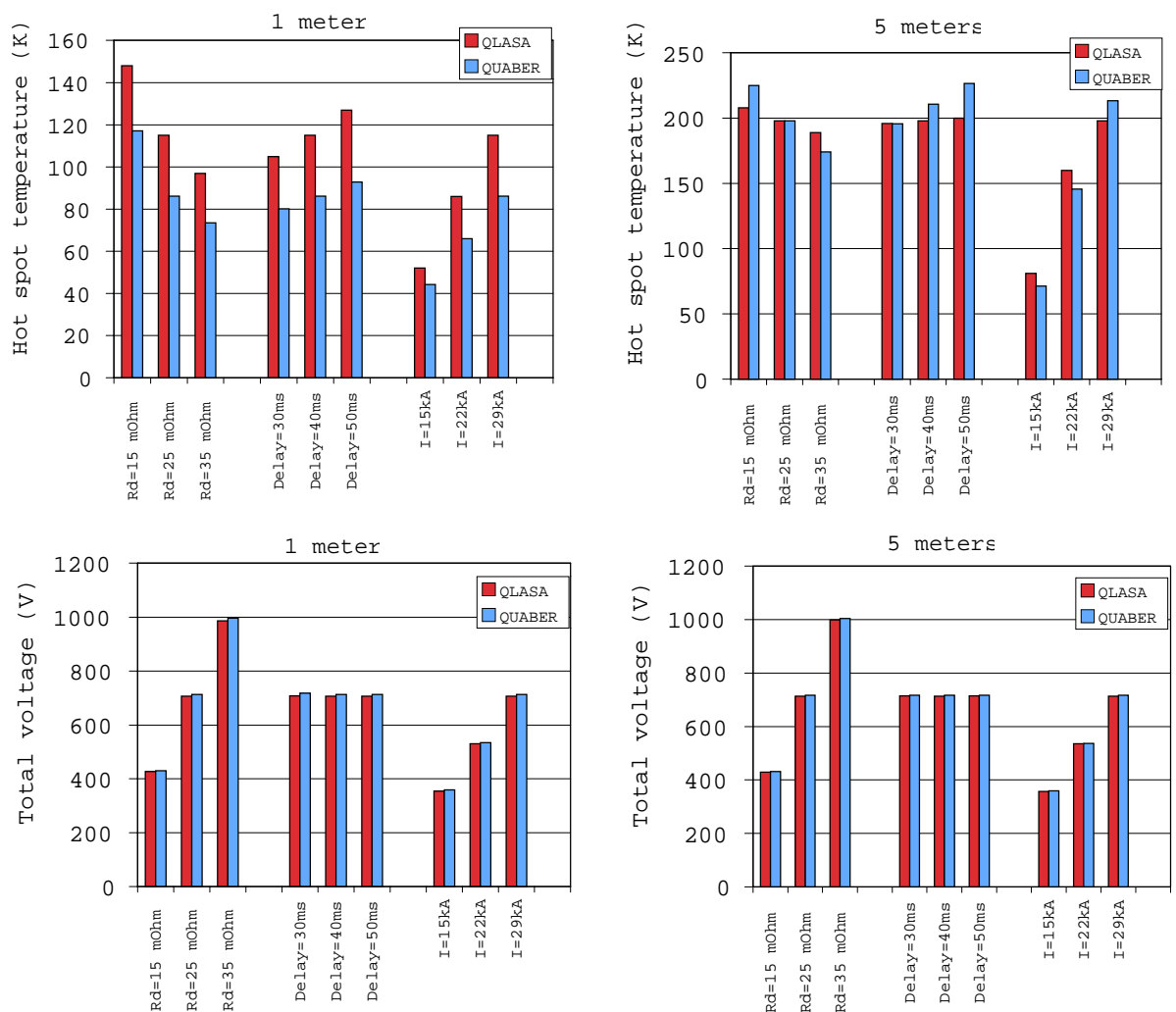
Fig. 45 Comparison of the hot spot temperature and the total voltage calculated with QUABER and QLASA for the cases of a 1-m and 5-m-long magnet.
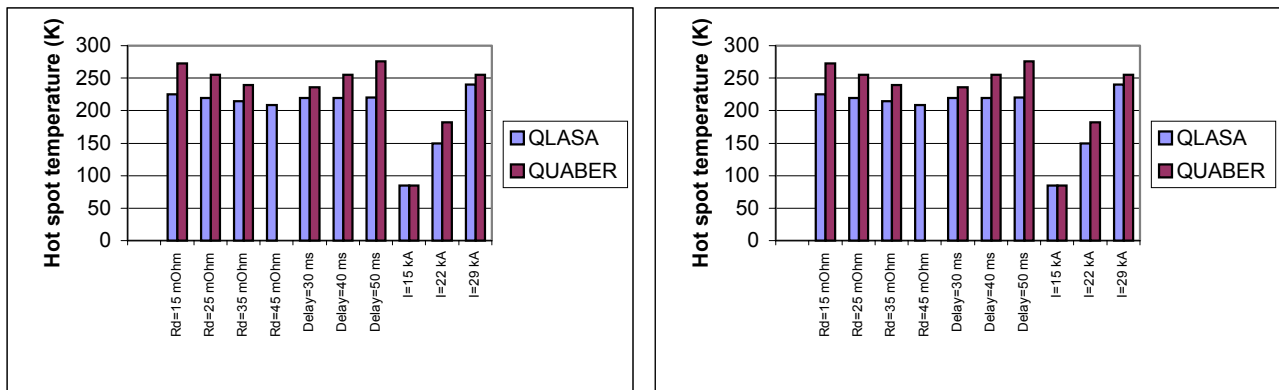
Fig. 46. Comparison of the hot spot temperature and the total voltage calculated with QUABER and QLASA for the case of a 10-m-long magnet.

The temperature behavior with respect to a change of the value of the dump resistance, of the heater and switch delays and of the operating current, computed by means of the two codes, is the same and the total voltages are nearly identical.

The discrepancy is on average 13% on the hot spot temperature and 0.5% on the total voltage. Let us point out that, for both codes, the total voltage is the product of the nominal current times the value of the dumping resistor, and this is the reason why the discrepancy in the total voltage is negligible. The two programs are conceived on similar theoretical basis but the quench propagation is modeled differently, which explains the discrepancy in temperature. QLASA is based on the resolution of analytical formulas to calculate the velocity of quenches in solenoids. QUABER is based on the resolution of differential equations for the equivalent electric circuit of the magnet once the value of the normal resistance is calculated at each time step (section 2).

5. CONCLUSIONS

In this report we have summarized the results of the simulations for the protection system of the NED dipole prototype. The simulations were performed with the programs QLASA and QUABER for 1-m, 5-m and 10-m-long prototypes. The results show that it is possible to protect the magnet, provided that heaters are used, at least for the 5 and 10 meter cases. In particular it is possible to keep the temperature below 300 K and the total voltage below 800 V with a dumping resistance of 25 mΩ and a heater delay of 40 ms.

The two programs (QUABER and QLASA) show a discrepancy on average of 13% on the hot spot temperature and of only 0.5% on the total voltage.

REFERENCES

[1]   L. Rossi, M. Sorbi, QLASA: a computer code for quench simulation in adiabatic multicoil superconducting windings, INFN/TC-04/13, July 2004.

[2]   M.N. Wilson, Superconducting Magnets, Claredon Press Oxford, (1983).

[3]   QUABER 2.0 Manual Utilisateurs, Version 1994

[4]   QUABER 4.0 user guide, F. Rodriguez–Mateos, F. Calmon, A. Marquis, R.Schmidt, LHC Project Note, 1997.

[5]   D. Leroy, O. Vincent-Viry, Preliminary Magnetic Designs for Large - Bore and High - Field Dipole Magnets, CERN/AT/2004-22, EDMS nr. 555826, Dec. 2004

[6]   Material Properties – Libraries Comparison – May 2004, LASA-report, CERN EDMS n. 555753

[7]   L.T. Summers, M.W. Guinan, J.R. Miller, P.A. Hahn, A model for the prediction of Nb_3Sn critical current as a function of field, temperature, strain and radiation damage, IEEE Trans. on Mag., Vol.27-2, 2041, (1991).

[8]   QUABER 4.0 user guide, F. Rodriguez–Mateos, F. Calmon, A. Marquis, R. Schmidt, LHC Project Note, 1997.

[9]   Saber, version 4.1.1, 1997, Analogy Inc. Beaverton, OR.

[10]   F.Sonneman, M.Calvi, Quench simulation studies: Program documentation of SPQR Simulation Program for Quench Research, LHC Project Note 265, July 2001.

APPENDIX A
SIMULATIONS WITH QLASA

Evolution of the current, voltages and hot spot temperature vs. the time for the 5-m and 10-m-long magnets, for a quench originating in the high field zone. The detection threshold voltage is 10 mV, the delay time of the quench heater and of opening of the main switch is 30 ms while the quench heaters cover the whole length of the magnet.

5-METER-LONG MAGNET
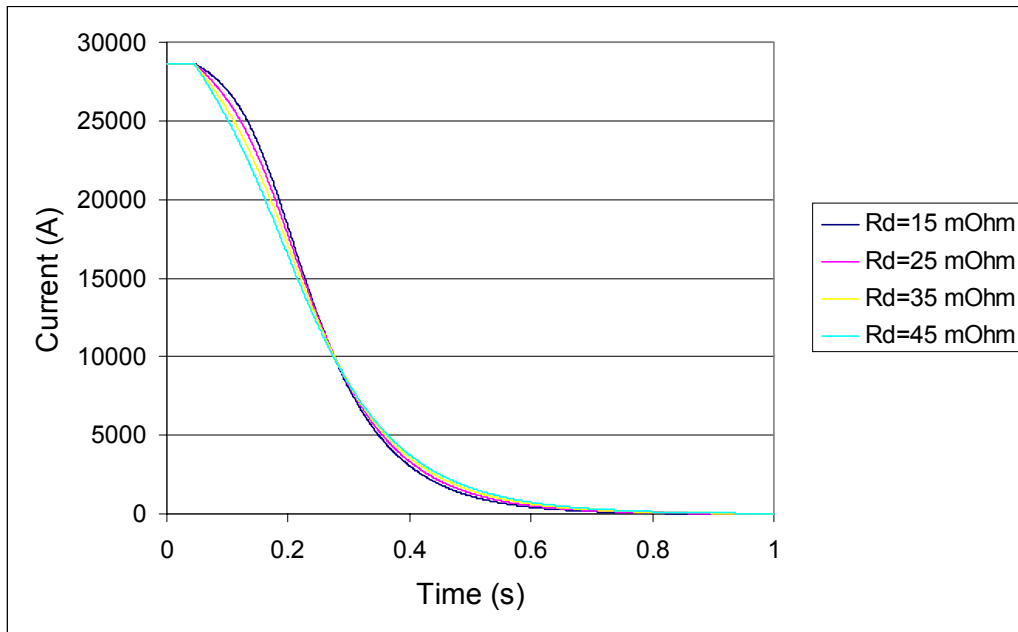
Fig. A1: Current decay for three values of dump resistance.
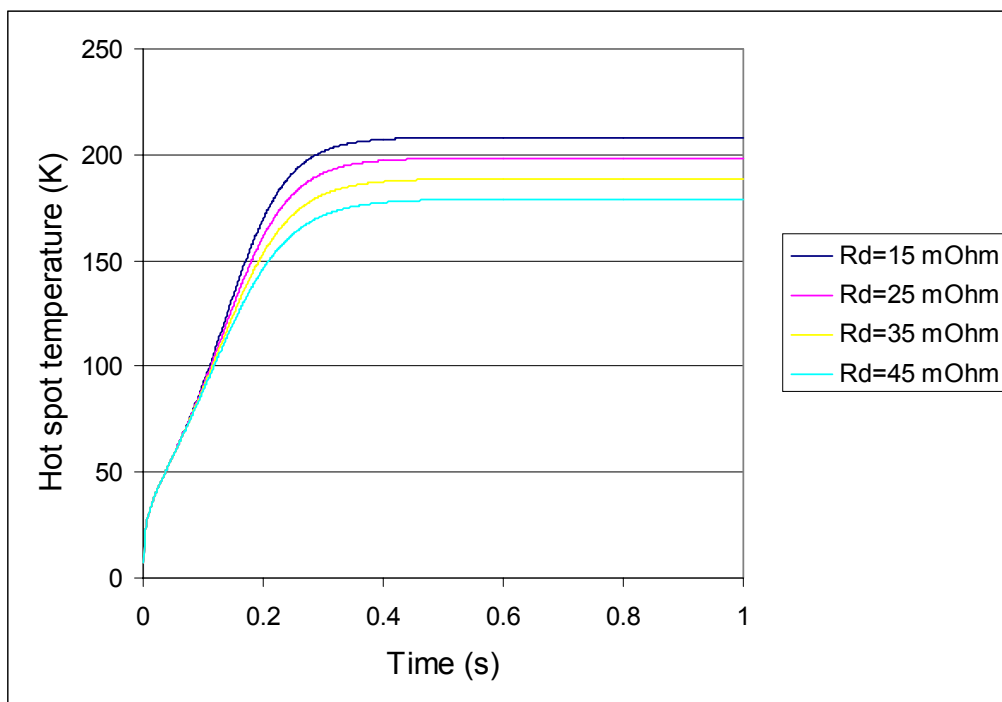
Fig. A2: Hot spot temperature for three values of dump resistance.
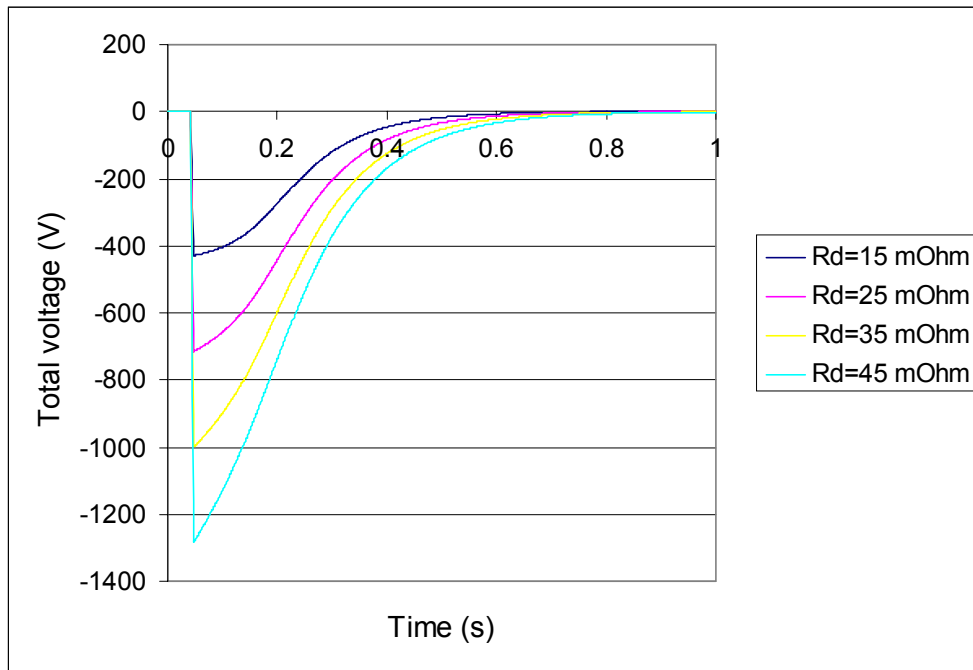
Fig. A3 Total voltage for three values of dump resistance.
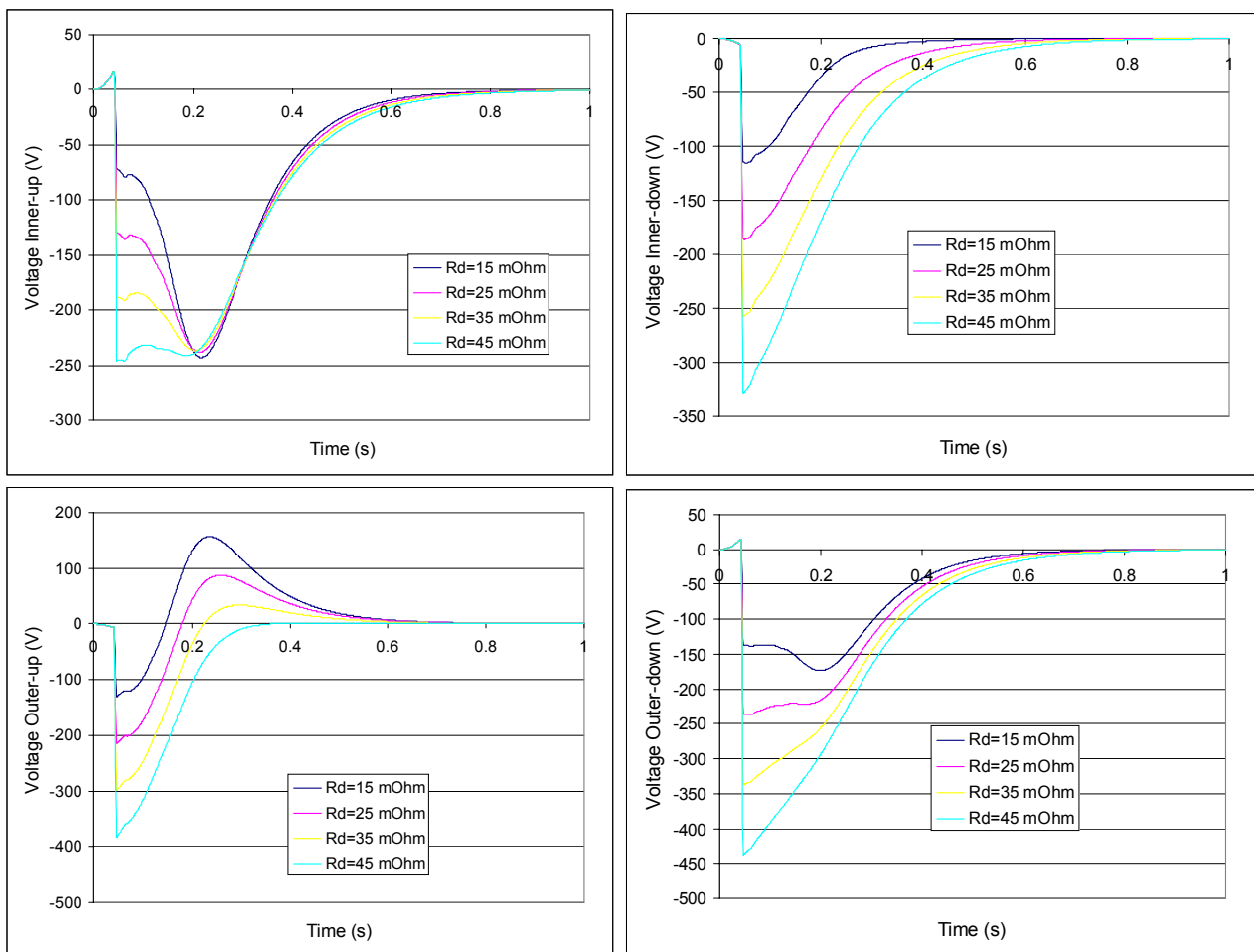
Fig. A4. Voltage across the four winding sectors for three values of dump resistance.

10-METER-LONG MAGNET
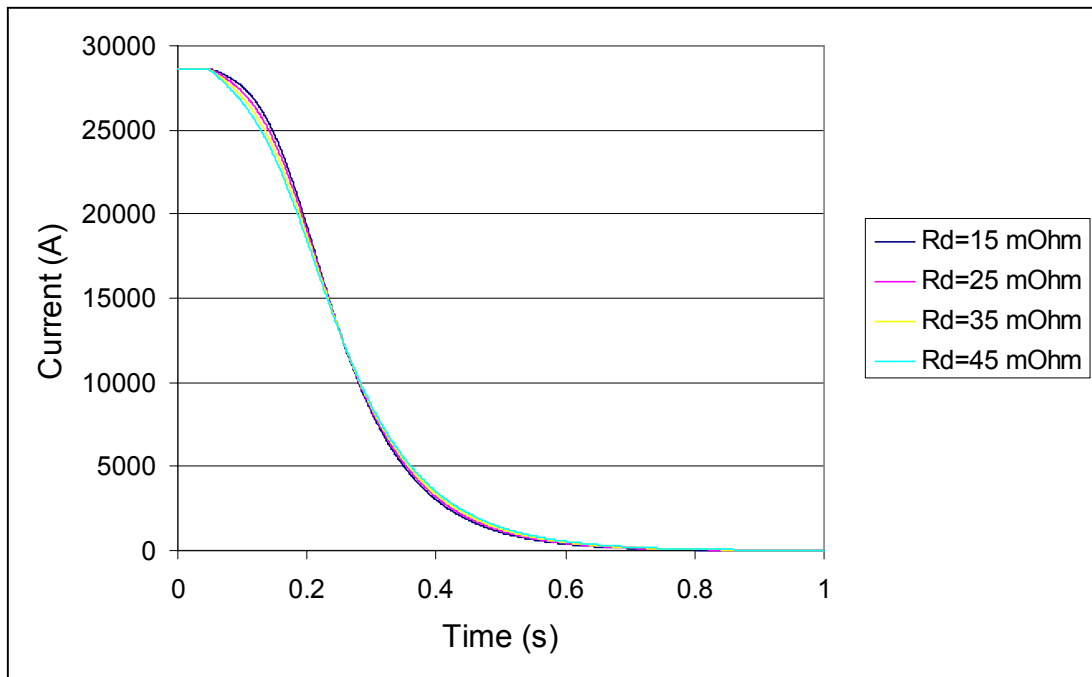
Fig. A5. Current decay for three values of dump resistance.
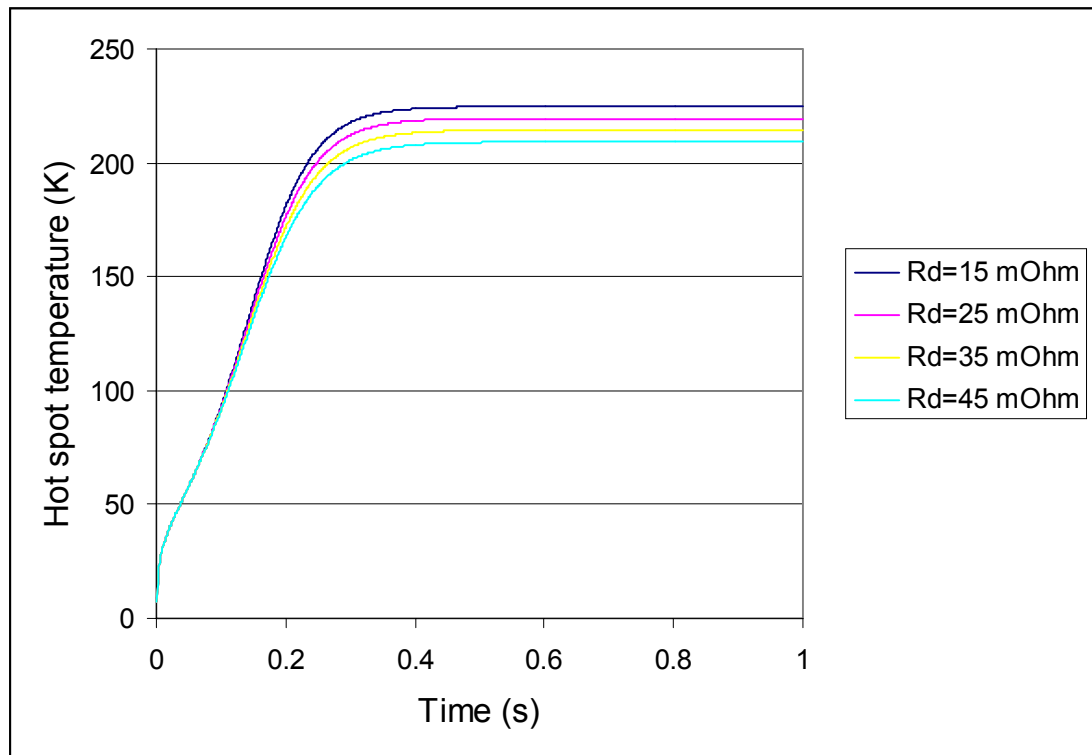
Fig. A6. Hot spot temperature for three values of dump resistance.
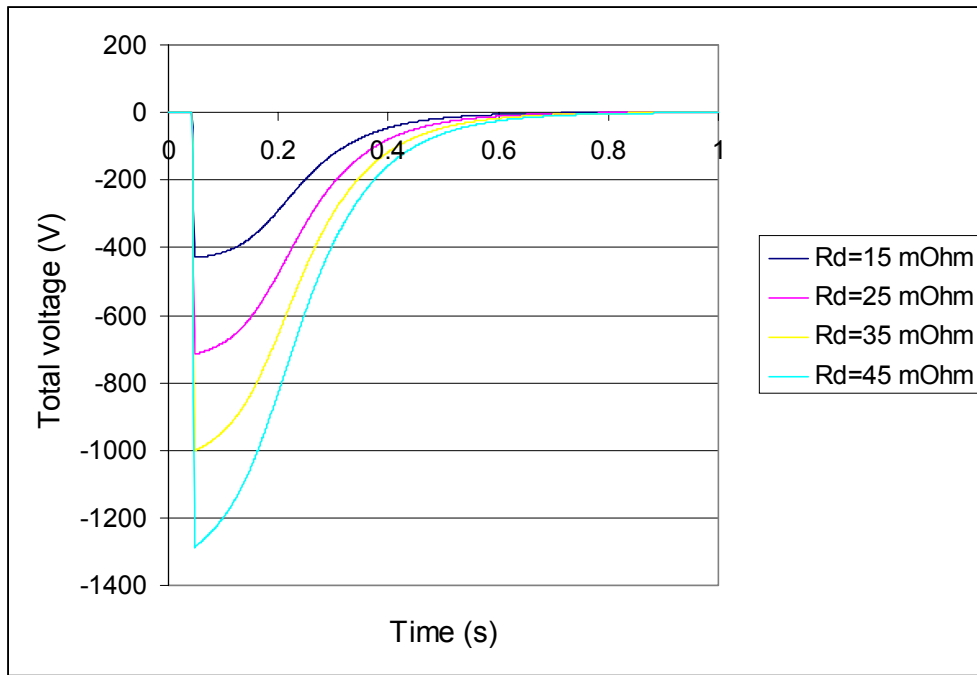
Fig. A7 Total voltage for three values of dump resistance.
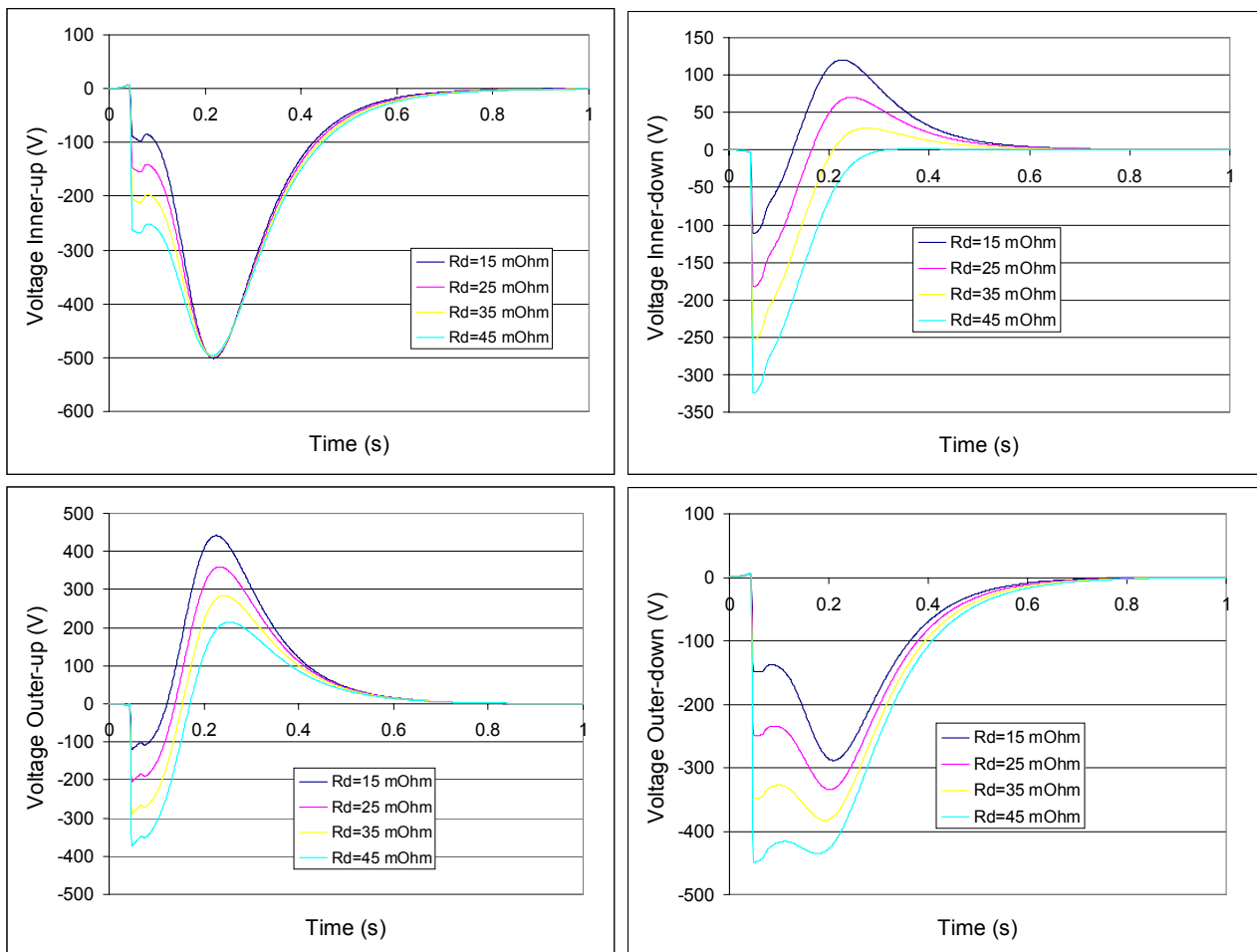
Fig. A8 Voltage across the four winding sectors for three values of dump resistance.

APPENDIX B
SIMULATIONS WITH QUABER

B.1   DUMP RESISTANCE

1-METER-LONG PROTOTYPE
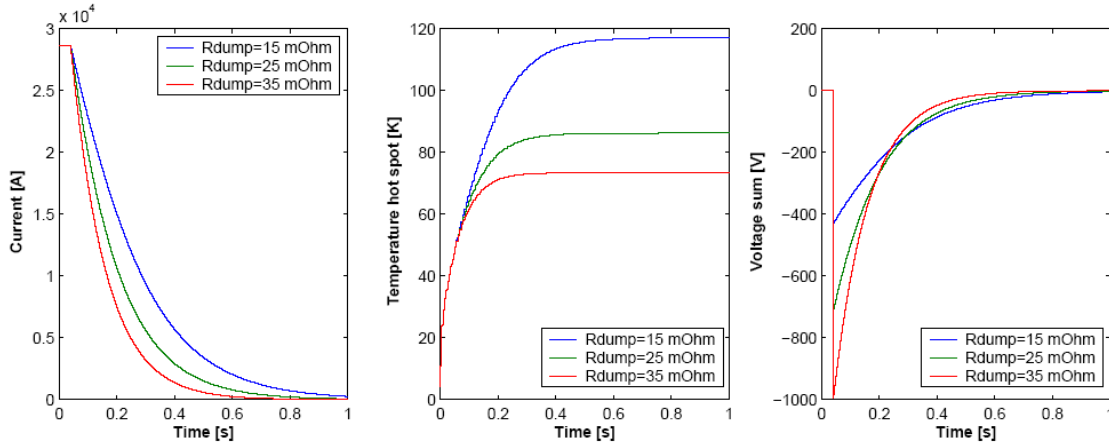
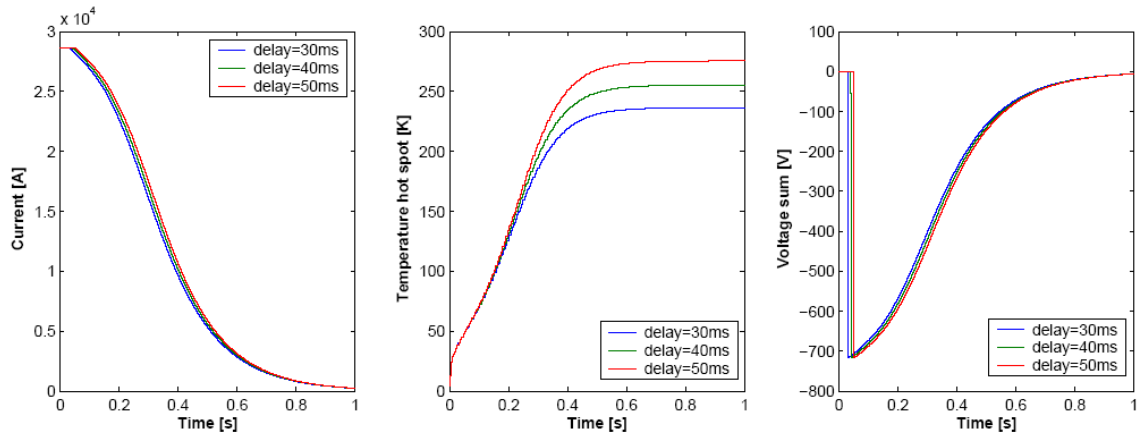Fig. B1 Current decay, hot spot temperature and total voltage for three values of dump resistance.
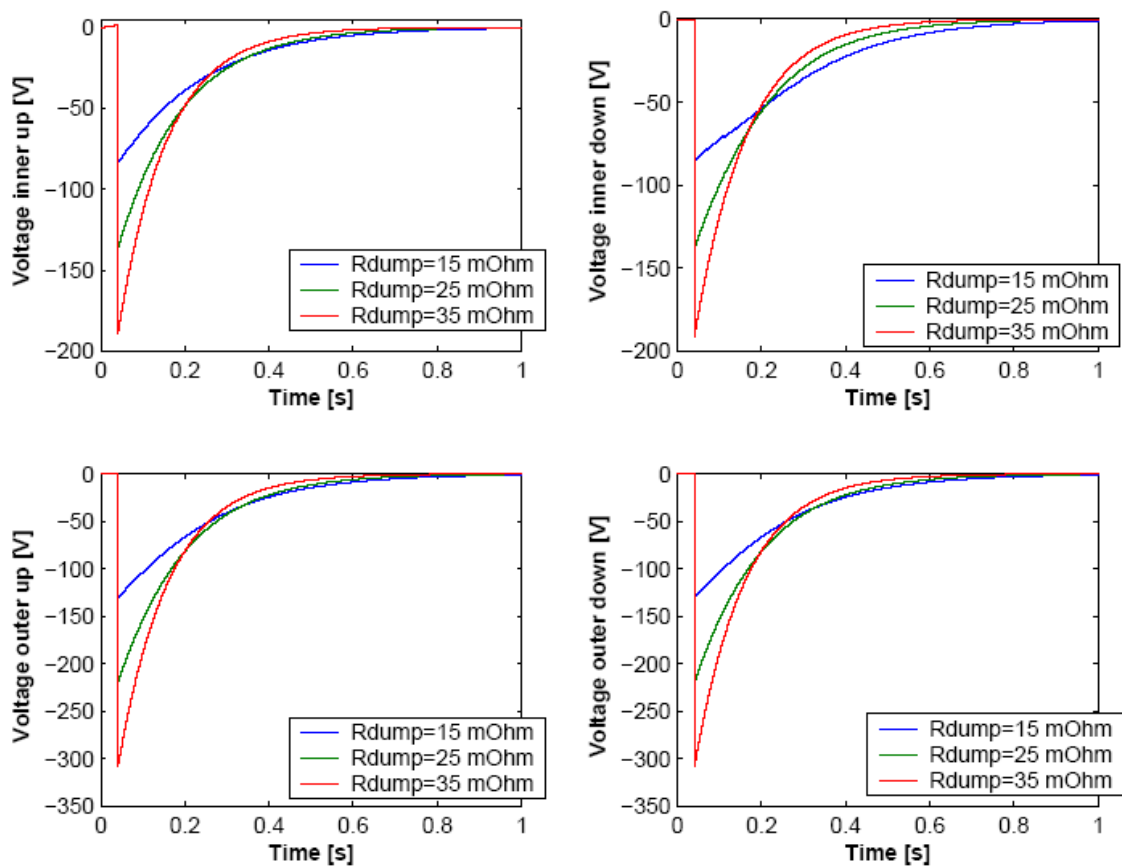
Fig. B2 Voltage across the four winding sectors for three values of dump resistance.

10-METER-LONG PROTOTYPE
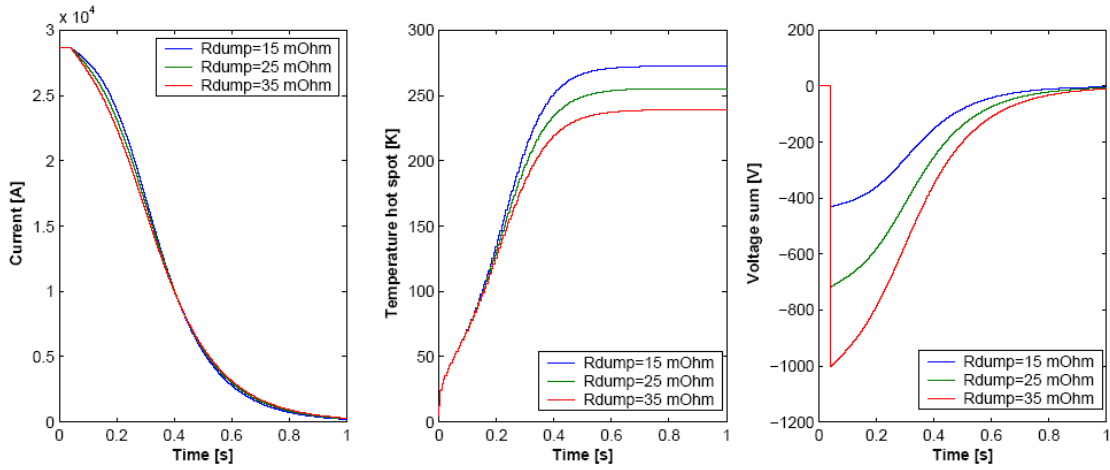
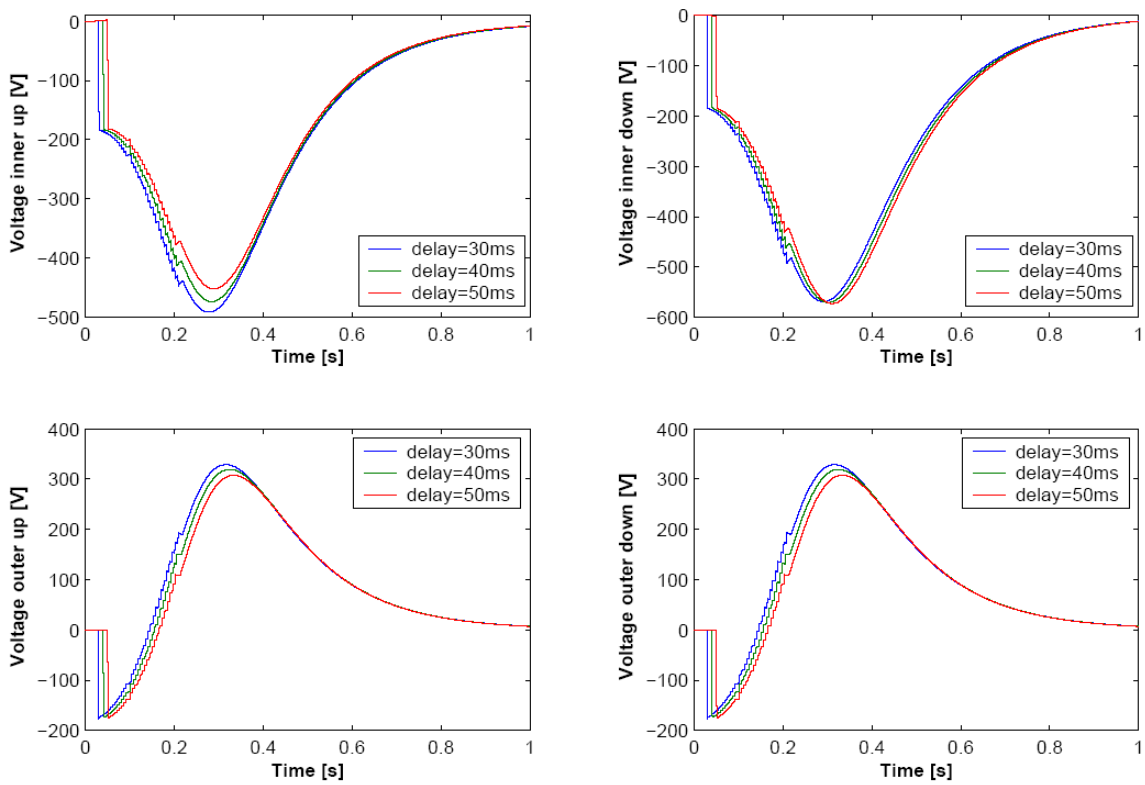Fig. B3 Current decay, hot spot temperature and total voltage for three values of dump resistance.
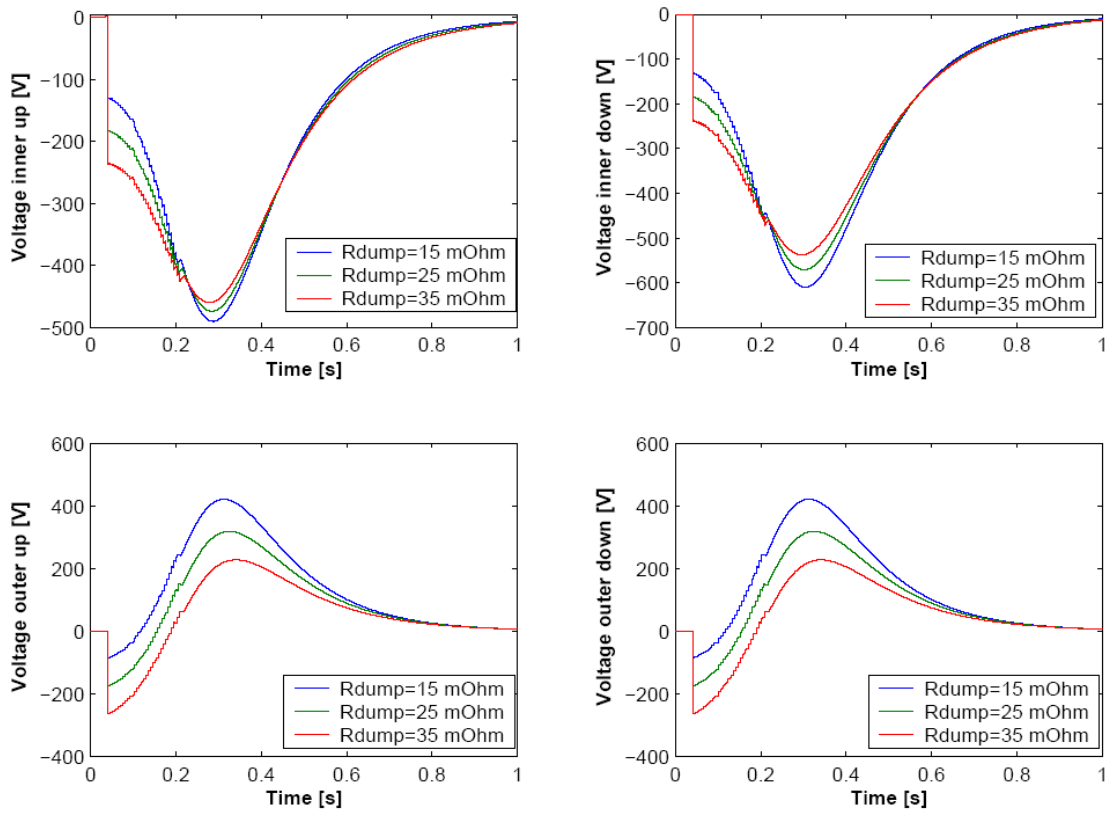
Fig. B4 Voltage across the four winding for three values of dump resistance.
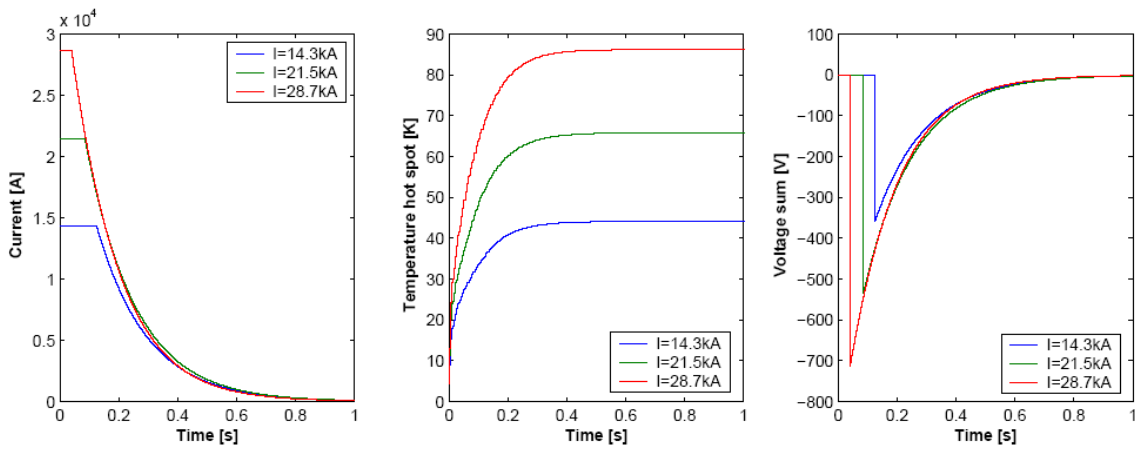
B.2   HEATER AND SWITCH DELAYS

1-METER-LONG PROTOTYPE
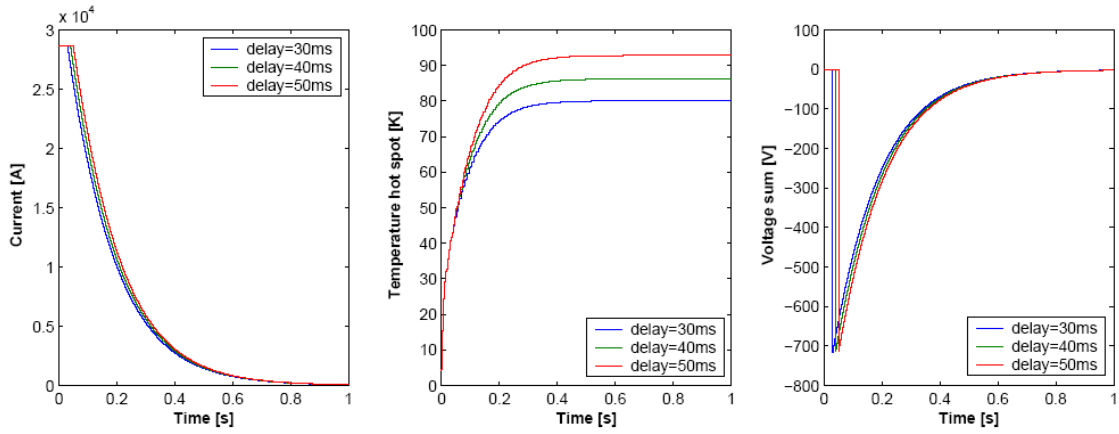
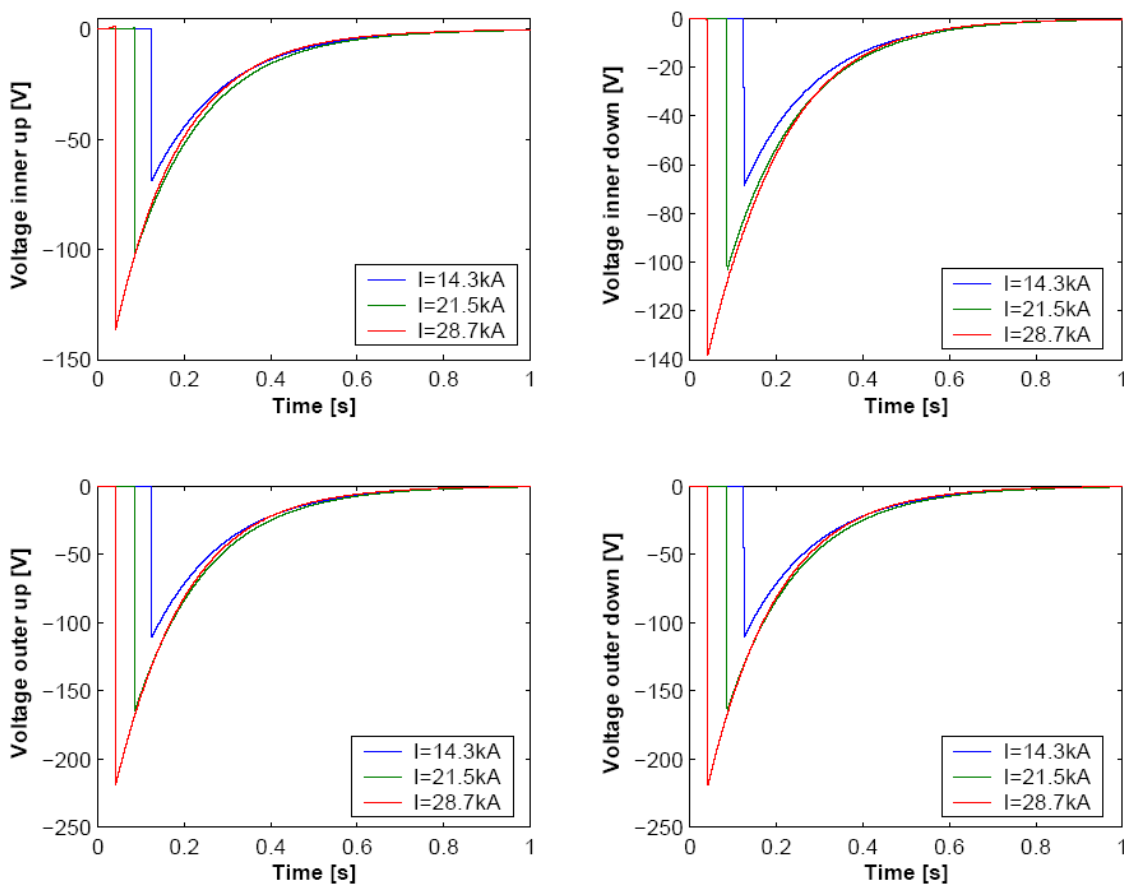Fig. B5 Current decay, hot spot temperature and total voltage for three values of delay time.
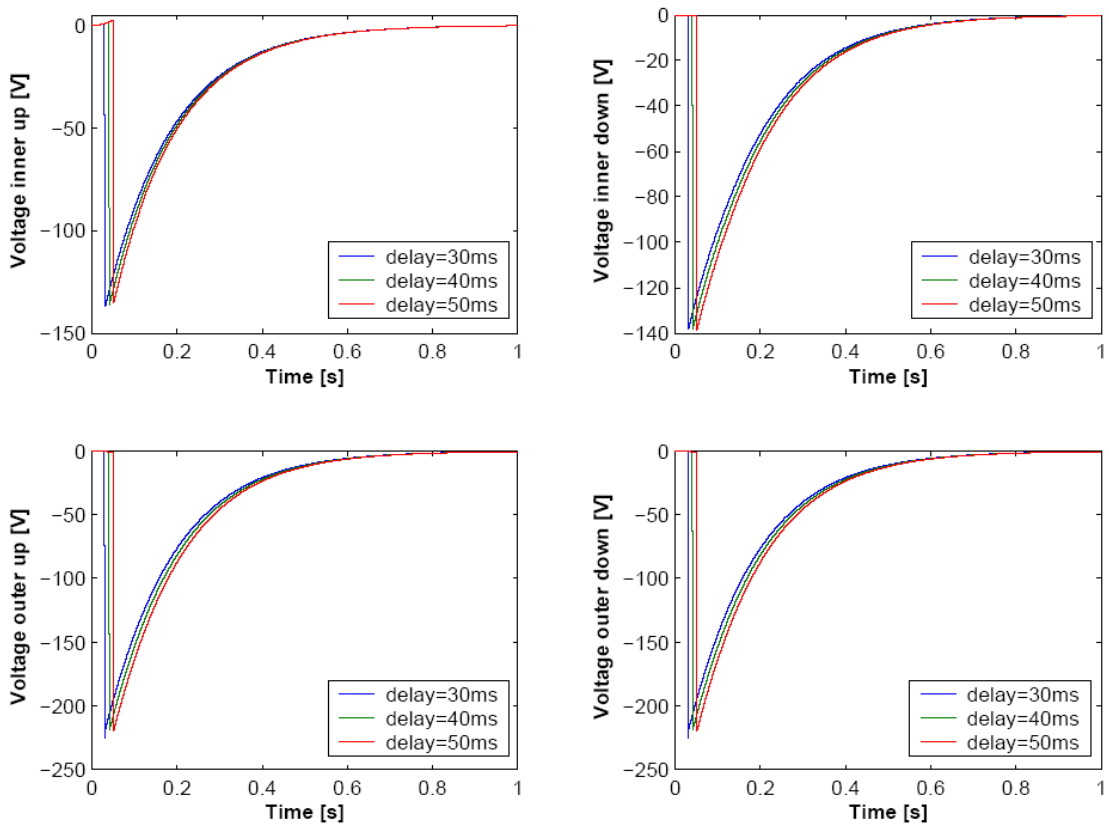
Fig. B6 Voltage across the four winding sectors for three values of delay time.

5-METER-LONG PROTOTYPE
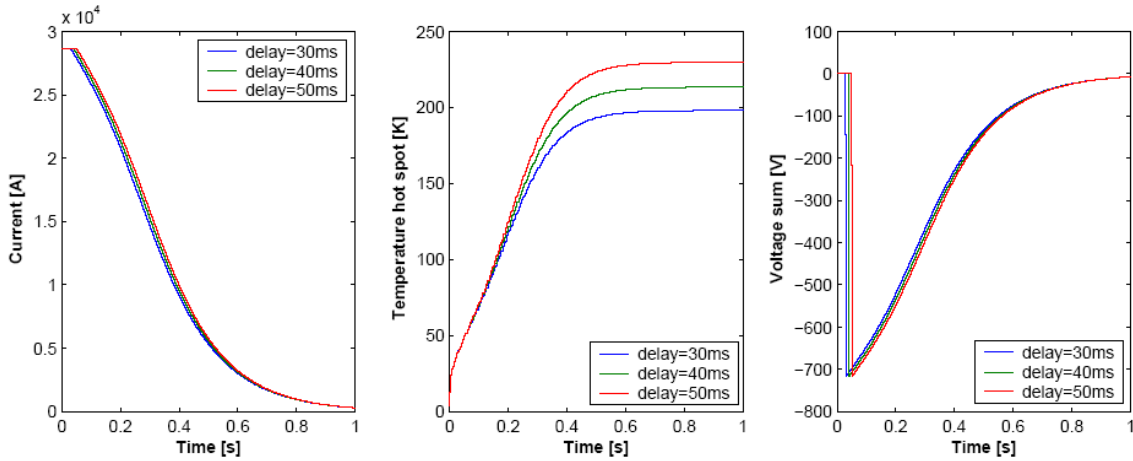
Fig. B7 Current decay, hot spot temperature and total voltage for three values of delay time.
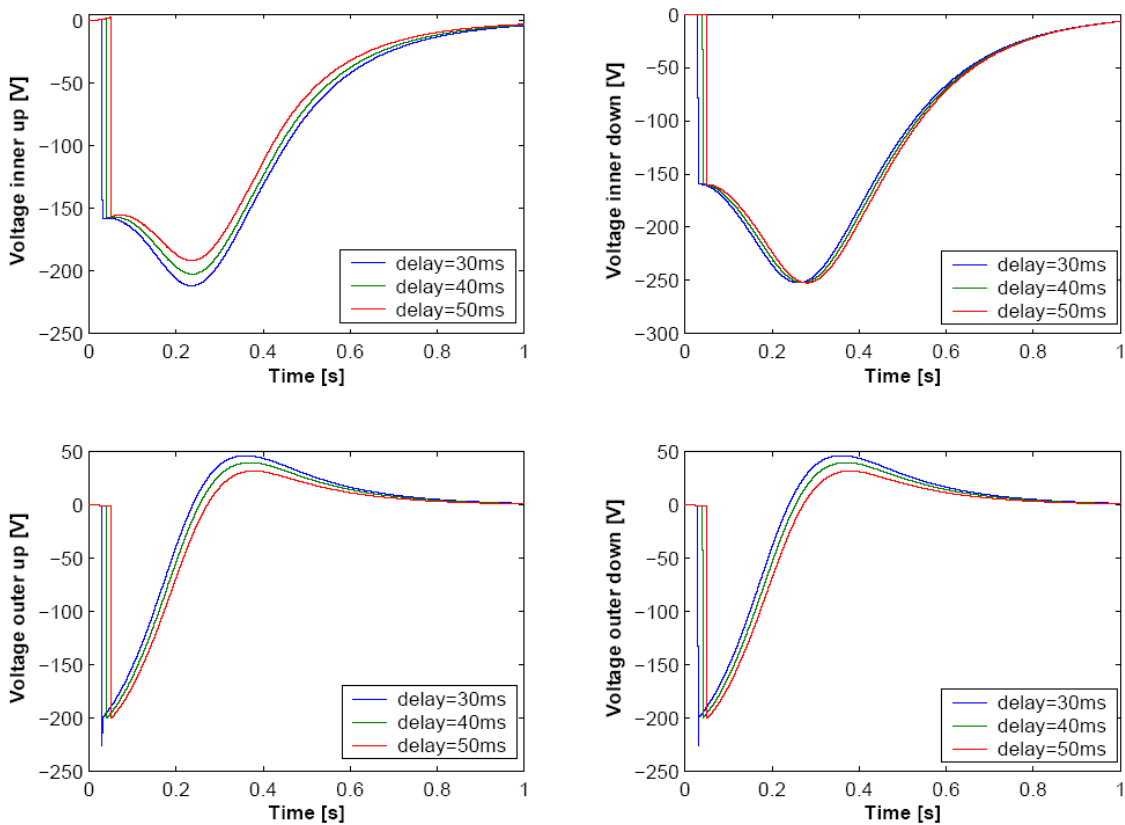
Fig. B8 Voltage across the four winding sectors for three values of delay time.

10-METER-LONG PRTOTYPE

Fig. B9 Current decay, hot spot temperature and total voltage for three values of delay time.

Fig. B10 Voltage across the four winding sectors for three values of delay time.

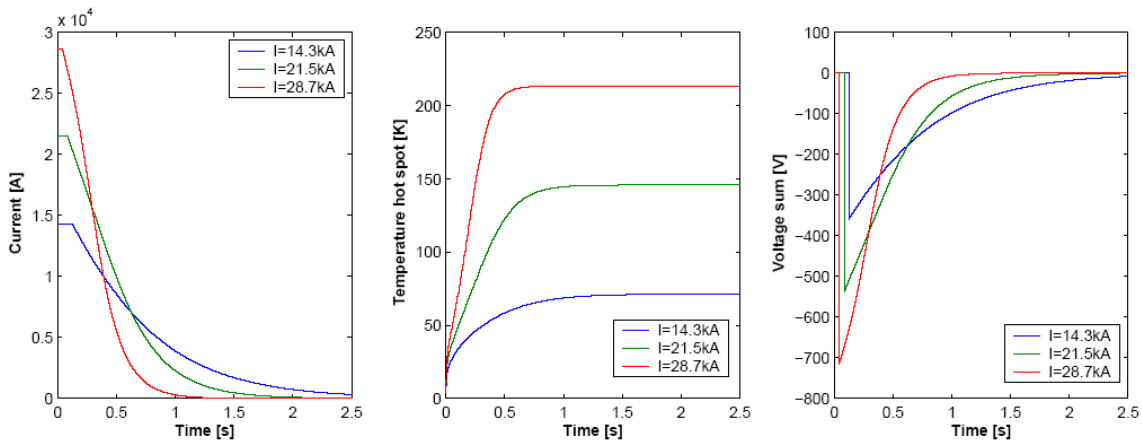## B.3   OPERATING CURRENT

1-METER-LONG PROTOTYPE

Fig. B11 Current decay, hot spot temperature and total voltage for three values of operating current.

Fig. B12 Voltage across the four winding sectors for three values of operating current.

5-METER-LONG PROTOTYPE

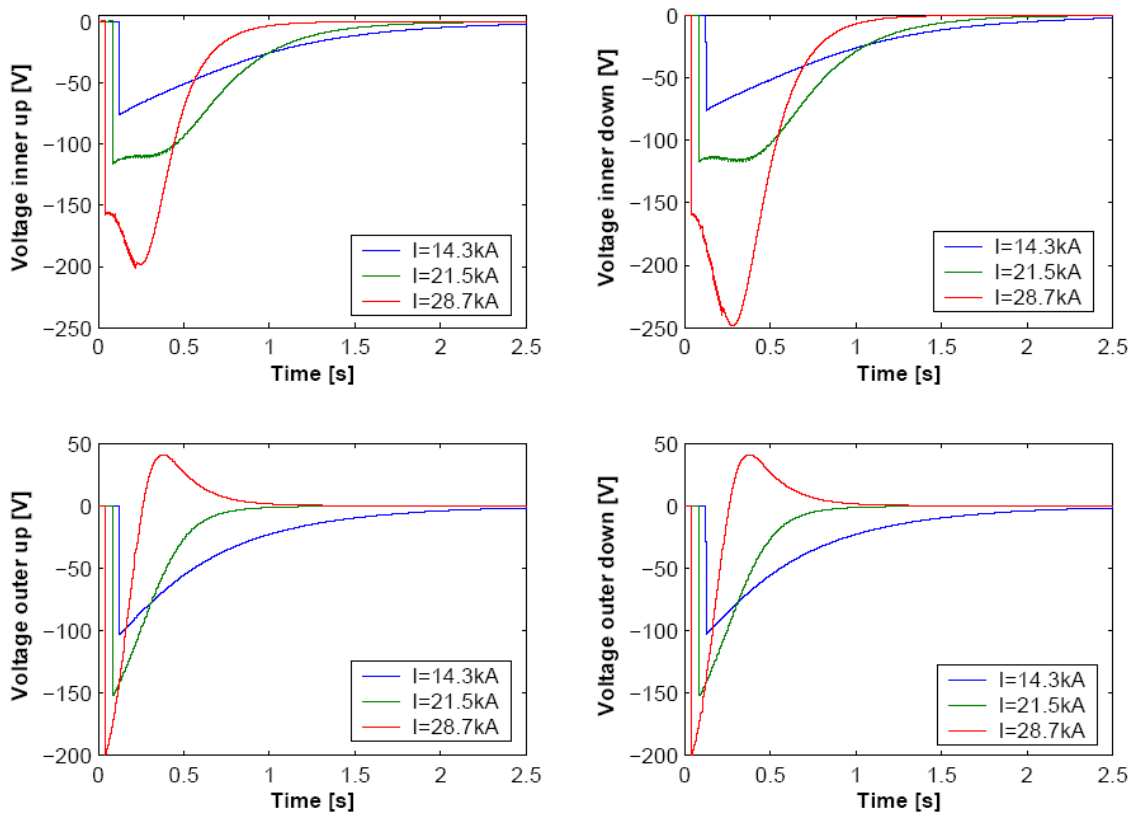Fig. B13 Current decay, hot spot temperature and total voltage for three values of operating current.

Fig. B14 Voltage across the four winding sectors for three values of operating current.
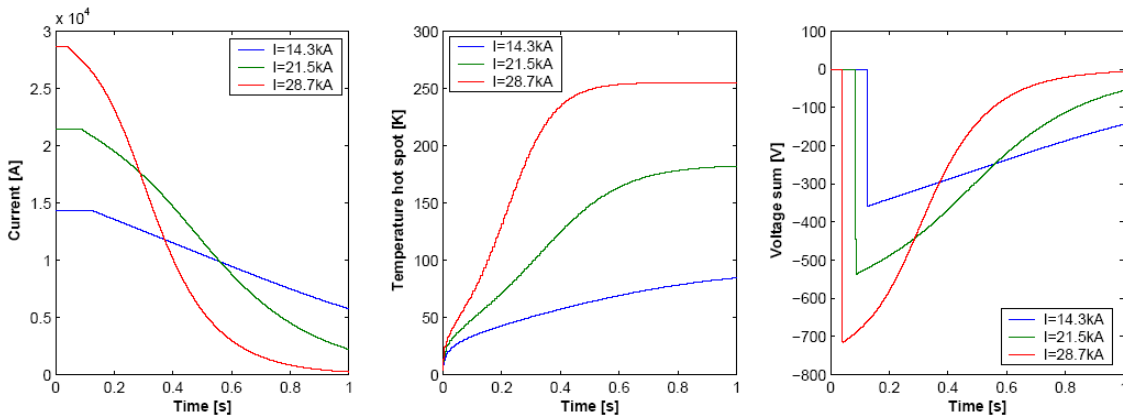
10-METER-LONG PROTOTYPE

Fig. B15 Current decay, hot spot temperature and total voltage for three values of operating current.
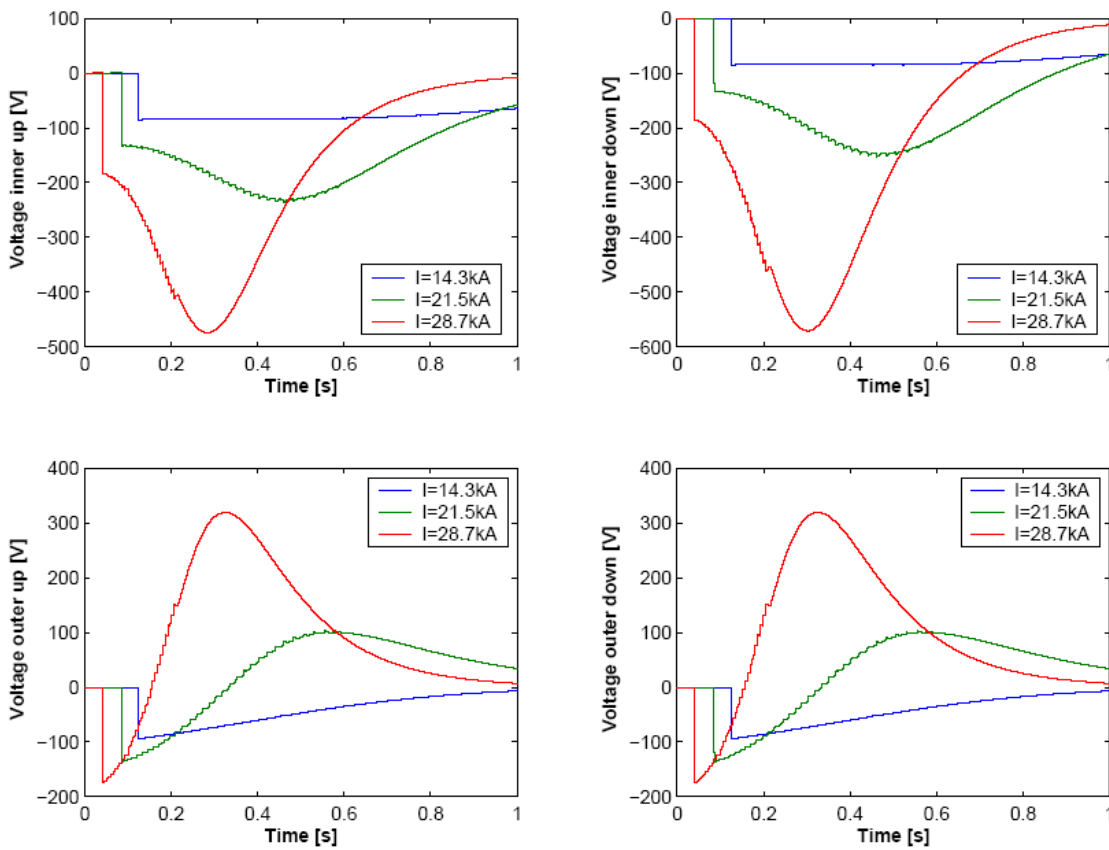

Fig. B16 Voltage across the four winding sectors for three values of operating current.